NAVAL POSTGRADUATE SCHOOL

MONTEREY, CALIFORNIA

THESIS

OPTIMIZING FUEL EFFICIENCY ON ISOLATED MICROGRID WITH ENERGY STORAGE SYSTEM UNDER VARYING LOADS

by

Joo W. Lee

June 2021

Thesis Advisor:	Emily M. Craparo
Co-Advisor:	Giovanna Oriti
Second Reader:	Arthur J. Krener

THIS PAGE INTENTIONALLY LEFT BLANK

REPORT DOCUMENTATION PAGE			Form Approved OMB No. 0704-0188

1. AGENCY USE ONLY *(Leave blank)*	2. REPORT DATE June 2021	3. REPORT TYPE AND DATES COVERED Master's thesis

4. TITLE AND SUBTITLE
OPTIMIZING FUEL EFFICIENCY ON ISOLATED MICROGRID WITH ENERGY STORAGE SYSTEM UNDER VARYING LOADS

5. FUNDING NUMBERS

6. AUTHOR(S) Joo W. Lee

7. PERFORMING ORGANIZATION NAME(S) AND ADDRESS(ES)
Naval Postgraduate School
Monterey, CA 93943-5000

8. PERFORMING ORGANIZATION REPORT NUMBER

9. SPONSORING / MONITORING AGENCY NAME(S) AND ADDRESS(ES)
N/A

10. SPONSORING / MONITORING AGENCY REPORT NUMBER

11. SUPPLEMENTARY NOTES The views expressed in this thesis are those of the author and do not reflect the official policy or position of the Department of Defense or the U.S. Government.

12a. DISTRIBUTION / AVAILABILITY STATEMENT
Approved for public release. Distribution is unlimited.

12b. DISTRIBUTION CODE
A

13. ABSTRACT (maximum 200 words)

Past studies of microgrid generator fuel efficiencies have been based on measurements of fuel consumption by generators under static loads. There is little information on fuel efficiency of generators under time-varying loads. To help analyze the impact of time-varying loads on optimal generator operation and fuel consumption, we formulate a mixed-integer linear optimization model to plan generator and energy storage system (ESS) operation to satisfy known demands. Our model includes piecewise linear fuel penalty terms on time-varying loads. We exercise the model on a number of scenarios and compare the resulting optimal fuel consumption and generator operation profiles. Our results show that the change in fuel efficiency between scenarios with the integration of ESS is minimal regardless of the imposed penalty placed on the generator. However, without the assistance of the ESS, the fuel consumption increases dramatically as the penalty imposed on the generator becomes greater. The integration of ESS shows a drastic improvement in fuel consumption, where the ESS allows the generator to minimize power output fluctuation to maximize fuel efficiency. The insignificance of penalty type and weight imposed on the generator provides potentially useful insight for future studies in developing a real-time controller.

14. SUBJECT TERMS
microgrid, isolated microgrid, optimization, energy storage, energy storage system, time-varying loads, fuel efficiency, fuel consumption, energy management system, energy management, forward operating base, microgrid generator, microgrid optimization, fuel efficiency performance, optimal energy scheduling, power production, penalty, generator penalty, fuel efficiency loss, linear penalty, piecewise linear penalty, integrated controller, microgrid controller, efficiency loss, power demand

15. NUMBER OF PAGES
73

16. PRICE CODE

17. SECURITY CLASSIFICATION OF REPORT	18. SECURITY CLASSIFICATION OF THIS PAGE	19. SECURITY CLASSIFICATION OF ABSTRACT	20. LIMITATION OF ABSTRACT
Unclassified	Unclassified	Unclassified	UU

NSN 7540-01-280-5500

Standard Form 298 (Rev. 2-89)
Prescribed by ANSI Std. 239-18

THIS PAGE INTENTIONALLY LEFT BLANK

Approved for public release. Distribution is unlimited.

OPTIMIZING FUEL EFFICIENCY ON ISOLATED MICROGRID WITH ENERGY STORAGE SYSTEM UNDER VARYING LOADS

Joo W. Lee
Ensign, United States Navy
BS, United States Naval Academy, 2020

Submitted in partial fulfillment of the
requirements for the degree of

**MASTER OF SCIENCE IN APPLIED SCIENCE
(OPERATIONS RESEARCH)**

from the

**NAVAL POSTGRADUATE SCHOOL
June 2021**

Approved by: Emily M. Craparo
Advisor

Giovanna Oriti
Co-Advisor

Arthur J. Krener
Second Reader

W. Matthew Carlyle
Chair, Department of Operations Research

THIS PAGE INTENTIONALLY LEFT BLANK

ABSTRACT

Past studies of microgrid generator fuel efficiencies have been based on measurements of fuel consumption by generators under static loads. There is little information on fuel efficiency of generators under time-varying loads. To help analyze the impact of time-varying loads on optimal generator operation and fuel consumption, we formulate a mixed-integer linear optimization model to plan generator and energy storage system (ESS) operation to satisfy known demands. Our model includes piecewise linear fuel penalty terms on time-varying loads. We exercise the model on a number of scenarios and compare the resulting optimal fuel consumption and generator operation profiles. Our results show that the change in fuel efficiency between scenarios with the integration of ESS is minimal regardless of the imposed penalty placed on the generator. However, without the assistance of the ESS, the fuel consumption increases dramatically as the penalty imposed on the generator becomes greater. The integration of ESS shows a drastic improvement in fuel consumption, where the ESS allows the generator to minimize power output fluctuation to maximize fuel efficiency. The insignificance of penalty type and weight imposed on the generator provides potentially useful insight for future studies in developing a real-time controller.

THIS PAGE INTENTIONALLY LEFT BLANK

Table of Contents

List of Figures

List of Tables

THIS PAGE INTENTIONALLY LEFT BLANK

List of Acronyms and Abbreviations

AMMPS	Advanced Medium Mobile Power Sources
CB-DDC	Contingency Base – Demand Data Collection
DoD	Department of Defense
ESS	energy storage system
FOB	forward operating base
gal	gallons
Hz	hertz
kW	kilowatt
kWh	kilowatt-hours
LIA	Logistics Innovation Agency
MILP	mixed integer linear program
min	minutes
PSO	particle swarm optimization
PV	photovoltaic
RTE	round trip efficiency
SOC	state of charge
TQG	Tactical Quiet Generator

THIS PAGE INTENTIONALLY LEFT BLANK

Executive Summary

Microgrid technological advancements have revolutionized warfighting capabilities by enabling long-term overseas operations. As a consequence, energy has become a crucial asset supporting Department of Defense missions. With increasing fuel costs, researchers have been developing new ways to conserve energy by designing new sophisticated controllers and upgrading power sources to increase microgrid fuel efficiency. A forward operating base (FOB) microgrid must be self-sustainable and cost-efficient because, as an isolated power system, it cannot rely on local power grids during wartime scenarios.

Previous research has focused on optimizing fuel consumption based on empirical generator efficiency data collected under static, steady-state loads. In reality, loads may be unpredictable and rapidly fluctuating. An important tool to mitigate the effects of rapid demand fluctuation is an energy storage system (ESS), such as a battery, which is integrated into the isolated microgrid architecture. The ESS allows the microgrid controller to effectively distribute power and communicate across the power-generating grid components to efficiently satisfy power demands and store excess generated power. The ESS also allows the integration of renewable power generators such as photovoltaic cells to reduce fuel consumption observed from traditional diesel generators.

This thesis builds on previous research to develop a microgrid controller designed to optimize generator fuel efficiency under time-varying demand scenarios. Specifically, we formulate a mixed integer linear programming optimization model to minimize fuel consumption while planning generator and ESS operations in such a way as to satisfy power demand. The objective function includes a penalty term designed to model generator efficiency loss as the generator's output fluctuates. We consider three different forms for this penalty term: no penalty, linear penalty, and piecewise linear penalty.

Using historical data collected from a U.S. FOB in the Middle East during 2014, we explore two case studies based on winter season power demand and summer season power demand to determine the optimal solution from the optimization model. Even though the average increase in power demand is approximately 15–20 kW from the winter season to the summer season, respectively, about 99% of all demand is satisfied by the generator during a 48-hour

optimization scenario when generator loss of efficiency is not considered in the model. We observe a decrease in generator output fluctuation as the penalty imposed on the generator increases, as the model uses the ESS to compensate for rapid fluctuations in power demand. As constant, steady-state generator output increases, the generator produces more power when a sudden decrease in power demand occurs, allowing the generator to charge ESS for future demands.

Regardless of the weights and types of the additive penalty imposed on the generator, we show that, on average, approximately 95–96% of all demand is satisfied by the generator and the remaining 4–5% of the demand is met by the ESS over a 48-hour optimization scenario. Even though the penalty term significantly impacts the optimal generator power profile, the change in the cumulative fuel consumption is insignificant. Additionally, we explore the effect of varying ESS round trip efficiencies (RTEs) over 240 different optimization models based on varying generator penalties and multiple 24-hour optimization scenarios. After experimenting with RTEs between 65% and 95%, we conclude that the effect of the RTE is insignificant. This study indicates about a 1–2% decrease in cumulative fuel consumption across the ESS RTEs.

The optimization model demonstrates the importance of taking the loss of generator fuel efficiency into account when analyzing power system performance under time-varying demands. Our results show a drastic change in optimal generator power production and ESS charging/discharging behavior as the magnitude of the penalty imposed on the generator increases. The power output of the generator fluctuates less which not only improves overall loss of fuel efficiency, but also lengthens the operational lifetime of the power system. It is critical for the microgrid architecture to include ESSs and implement fuel efficiency loss into the fuel consumption calculation so that the controller ensures a smoother generator power output when the power system experiences significant time-varying power demands.

Acknowledgments

This thesis would not have been possible without the tremendous support that I have received throughout my academic career. I would like to express my gratitude to all my teachers, professors, mentors, family members, and friends who have challenged, supported, and never gave up on me through this arduous academic journey.

I would first like to thank Dr. Emily Craparo and Dr. Giovanna Oriti for their inspirational leadership and invaluable expertise in the technical field throughout my thesis journey. I have learned so much about using my previous electrical engineering background to formulate and analyze optimization models. The utmost patience and guidance that I have received from my advisors is indescribable as I struggled to juggle thesis research, class assignments, and personal life. This thesis would not have been possible without their time and dedication to my success.

Additionally, I would like to express my appreciation to Dr. Arthur Krener for his extraordinary insight and technical expertise. He has challenged me to think critically: he would always push me to think beyond the specific problem. Thank you for expanding my mathematical and technical writing skills to help me become a better researcher.

Lastly, I would have not made it thus far without the overwhelming support from my family, friends, and mentors. My family has always been beside me throughout my entire academic journey. They have always pushed me to perform at my best and never gave up when faced with difficult situations. Thank you Mom, Dad, and Sung-Won. To my immediate NPS curriculum cohort friends: You are my family away from family. I will never forget the spontaneous get-togethers, late night study sessions, and wild weekend adventures. I could have not gotten through this program without the immense amount of motivation and support I received from you. As always, we are all in this together!

THIS PAGE INTENTIONALLY LEFT BLANK

CHAPTER 1:
Introduction

Demand for energy is increasing significantly as new innovations in technological warfighting capabilities are more readily available. As warfighting transitions into the cyber and space domains, energy "has been and will remain a fundamental enabler of military capability" according to the U.S. Office of Assistant Secretary of Defense for Energy, Installations, and Environment (Office of the Assistant Secretary of Defense for Energy, Installations, and Environment 2018a). With the expansion of deployed military operating bases in the world, military organizations need reliable and sustainable microgrid power systems to effectively generate energy required for various operations, such as training and sustaining military forces in remote locations.

The importance of energy to the Department of Defense (DoD) is captured in the term "operational energy." The U.S. Code 2924 Section 5, which went into effect in January 2012 and was updated in 2018, defines operational energy as "the energy required for training, moving, and sustaining military forces and weapons platforms for military operations" (United States Code 2018). Operational energy is considered to be one of the most essential components of warfighting for all military service branches. The National Defense Strategy published in 2018 outlines that the capability to fight and win future wars hinges on the ability to maintain and sustain new technologies such as advanced computing and big data analytics (Department of Defense 2018). The ability to manage energy-consuming equipment, such as newly developed weapons, translates into the importance of improving operational costs for future theaters. The Office of the Assistant Secretary of Defense for Sustainment outlines that the DoD "consumed over 85 million barrels of fuel to power ships, aircraft, combat vehicles, and contingency bases at a cost of nearly $8.2 billion" in fiscal year 2017. This further emphasizes the importance of "mitigating risk and cost in the supply and use of energy in operations and training" (Office of the Assistant Secretary of Defense for Energy, Installations, and Environment 2018b). It is imperative to ensure that each forward operating base (FOB) has cost-effective and efficient microgrid power system to generate the energy that is needed to successfully fight and defend against adversaries.

1.1 Microgrid

When temporary military bases are built in forward operating areas such as the Middle East, self-sustainability is one of the most important features to take into account, as one cannot rely on local power grids. The FOB must become self-sufficient and produce its own energy efficiently and cost-effectively. A FOB functions as an "islanded grid," meaning that it relies on its generators and energy storage system (ESS) to satisfy its power demand.

A microgrid is a fully functioning, self-sustaining power system that does not require an outside power grid to help satisfy its respective power demands. In other words, a microgrid is formed when an electrical grid is capable of operating as an island isolated from the main grid (Katiraei et al. 2005). A microgrid is broken down into generators, ESSs, and loads that need to be met. In many cases, when fuel is not readily available, microgrids are reliant on renewable energy sources such as wind turbines and solar photovoltaic (PV) cells, in addition to the standard diesel generators. Additionally, the ESS is a useful tool that assists the generators to run more efficiently by providing energy during the most strenuous time periods; however, the storage systems increase microgrid control complexity, as the microgrid controller must calculate the optimal power flow balance between using the generators and ESSs (Morstyn et al. 2018). The ESS in the microgrid can take the form of batteries, fly wheels, supercapacitors, or other devices. As microgrids are intended to be self-sufficient, the ESS is one of the primary ways to ensure that the system is stabilized against fluctuating loads and unmanaged energy sources such as wind turbines (Hartono et al. 2013).

Modern microgrids with an integrated ESS have sophisticated controllers that act as a central command unit. The controller is able to optimally distribute power demands between the generator and the ESS, as it ensures that all critical loads are met during all microgrid operating modes (Hartono et al. 2013; Ton and Reilly 2017). The controller dispatches power to the various entities to ensure that power demand is consistently met between the generator and ESS in the most efficient way possible. In doing so, the controller improves reliability, reduces cost, and diversifies power generation while maintaining power delivery to the most critical electrical loads.

1.2 Static vs. Time-Varying Load

A predominant issue that operational microgrids usually face is the unknown state of the future power demands. Previous studies have shown that microgrids are able to handle static, constant loads for a long period, as generators do not need to ramp up and down to meet fluctuating power demands (Garcia 2017; Bhandari et al. 2013). With a steady-state power demand, the stress on the microgrid is less. However, in reality, loads change over time, sometimes very rapidly.

To mitigate the effects of fluctuating loads, Sprague researches an optimization approach to coordinate generators and environmental control units in such a way as to maximize generator efficiency by running the generators at higher loads. A generator's efficiency is maximized at its rated power, so Sprague develops an optimization approach designed to run the generator at higher speeds even during non-peak hours so time-varying load occurrences are observed as static loads when additional power is produced.

Without implementing Sprague's load scheduling technique, the transition between static load and time-varying load introduces generator power instability (Ahmed et al. 2017). Uncertainty of future power demand and the consistent stress on the microgrid power generators cause microgrid instability. Therefore, the controller tries to meet the power demands regardless of drastic power fluctuation. As a result of complex microgrid power demand complications, the controller becomes one of the most important elements of the microgrid, as optimal power scheduling becomes more relevant when trying to successfully meet all time-varying load requests (Fakhrazari et al. 2014).

1.3 Fuel Efficiency

Past studies of generator fuel efficiency have been based on measurements of generator fuel consumption under static loads. In reality, loads are changing, and to our knowledge there has been no empirical study of generator fuel efficiencies under time-varying loads. Previous studies address microgrid generator optimization, fuel consumption efficiency, and microgrid integrated energy storage efficiencies; however, these studies are based on generator fuel consumption measurements collected under static load (Garcia 2017; Kiser 2018).

In this thesis, we introduce a generator penalty term designed to model a loss of efficiency as generator output fluctuates. Based on the rate of change of generator throttle setting, the penalty term varies the overall generator fuel consumption. We include an ESS in our notional microgrid to allow the generator to produce a more constant output, despite fluctuating demand.

We use two different approaches to impose penalty terms for time-varying loads. First, we use a linear approach where the fractional change in generator power multiplied by a predefined scalar penalty coefficient is directly added to the cumulative fuel consumption. Second, we use a piecewise linear approach to vary the penalty coefficient based on the fractional change in generator power.

1.4 Thesis Organization

This thesis is organized as follows. Chapter 2 provides an overview of the large body of research related to minimizing fuel consumption and maximizing fuel efficiency on microgrids. As the topics related to microgrids have been skyrocketing in popularity, many studies have been conducted using various optimization models, different approaches to energy scheduling with the use of ESSs, and variations of microgrid architectures. This chapter highlights the key topics in order to provide a foundation to better explain the importance of imposing a penalty on the generator.

Chapter 3 describes the microgrid architecture and mixed integer linear program (MILP) optimization model that are considered in this thesis. Based on generator characteristics, ESS details, and power demands, the optimization model prescribes the optimal contribution of each microgrid energy resource at a given time. Chapter 3 also explains the unique methodologies that introduce the additive linear penalty and the additive piecewise linear penalty.

Chapter 4 exercises the model on several case studies and highlights insights gained from these instances.

Finally, Chapter 5 presents the conclusion and final thoughts from this study, as well as various recommendations for future research areas.

CHAPTER 2:
Background and Literature Review

Studies of microgrid operations are increasing as countries realize the effectiveness of modeling military operating bases overseas as microgrids. As more research is conducted on microgrids, many scholarly articles, journals, and books on microgrid research are readily available. Previous studies explore different approaches to vary the architecture of microgrids, find unique ways to optimally schedule energy distribution, and formulate optimization models. Researchers have made it a point to optimize microgrids so that they are cost effective and reliable to deploy, and many studies use fuel consumption as their main measure of performance.

2.1 Microgrid Architecture Variation

The two main energy resources that make up an islanded microgrid architecture are the generator(s) and the ESS. It is important to determine the correct size of these resources in a microgrid to meet the power demand at any given time. Gamarra and Guerrero explain that generator as well as energy storage selection and sizing affect the microgrid's fuel consumption, and that the energy resources must be sized in accordance to their peak-load demand criteria (Gamarra and Guerrero 2015). By considering the various load types, fuel suitability, and the initial investment made to establish the microgrid, the best possible power system to satisfy future power demand requires extensive research in the selection of the energy resources that make up the architecture. For example, Kazem and Khatib indicate that an optimal hybrid PV/wind/diesel generating system combination can be identified by a sizing algorithm based on power supply availability, cost of each power generating component, and power system design specifications (Kazem and Khatib 2013). The algorithm determines the optimal sizing ratio for each energy resource based on the expected power demands.

Katiraei and Abbey determine the size of a generator by analyzing past daily and seasonal load fluctuation and, most importantly, by incorporating constraints of a diesel generator in operation (Katiraei and Abbey 2007). The sizing is obtained through a dynamic energy flow

model where smaller diesel generators can be used if newer renewable energy sources are integrated into the microgrid. Katiraei and Abbey suggest that with the fast reactive power compensation from the diesel generator caused by power fluctuation, larger generators are necessary to compensate for the sudden power change created by renewable power sources such as wind turbines (Katiraei and Abbey 2007).

In addition to generator sizing, Ulmer conducts research on microgrids by implementing renewable energy sources into the architecture. Ulmer takes past weather information such as solar and wind data to design a microgrid in order to maximize the microgrid's "islanding time," defined as the time the microgrid can operate in a self-sufficient manner without external fuel supplies or connection to a main power grid (Ulmer 2014).

As generator overloading has been a common microgrid failure, more technologically advanced microgrids have integrated ESS that must be taken into consideration. A disadvantage of an ESS is the initial investment cost; however, generation power shortages can be mostly combated with integrated storage. As larger ESSs become exponentially expensive in cost, Bahramirad et al. present a sizing methodology for ESS integration using MILP to choose an optimal storage size by taking initial investment costs and microgrid operating costs into account (Bahramirad et al. 2012). Bahramirad et al. conclude that ESSs have economic benefits, a practical use when integrated into the architecture, and an ability to make the microgrid much more reliable during higher power demands (Bahramirad et al. 2012).

Similar to the study conducted by Bahramirad et al., Chen et al. present a different approach on sizing the energy storage in microgrids by introducing a cost-benefit analysis to optimally size storage units. By designing multiple microgrid architectures, Chen et al. use forecast data to minimize the total cost of a microgrid while maximizing the total benefits through an MILP technique (Chen et al. 2012). This approach identifies the optimal ESS by using statistical forecasting techniques to determine the wind speed and solar radiation of a particular day to perform a cost-benefit analysis. Using this approach, the study shows that when the size of the ESS increases, either the benefits increase or the cost decreases until the rate of increasing benefits and the rate of decreasing cost become insignificant (Chen et al. 2012).

An important takeaway from islanded microgrid studies is that generator as well as energy

storage size and capacity have a significant impact on fuel consumption and operational costs. In order to mitigate the unnecessary costs, the size of these energy resources should be determined by using optimization techniques such as cost-benefit analysis and machine learning approaches.

2.2 Optimal Energy Scheduling Techniques

The concept of optimal energy scheduling improves energy utilization while minimizing generator fuel consumption costs in a microgrid. Several studies present optimal energy management systems for microgrids by tuning the controller which determines the power flow within the system. Some of these studies examine the performance of microgrids with and without ESS. Moradi et al. report the difference in optimal energy scheduling in a microgrid with and without ESS, concluding that the integration of ESS saves a significant amount of fuel compared to a microgrid without an energy storage unit (Moradi et al. 2017). Continuing the exploration of optimal energy scheduling techniques, Liu et al. experiment with various microgrid operation modes including utility grid-connected mode and off-grid operation mode using a day-ahead scheduling optimization technique to minimize fuel cost (Liu et al. 2020). The studies conducted by both Moradi et al. and Liu et al. show the consistency of prioritization given to loads with a higher power demand to minimize power loss. The demand is mostly satisfied by the ESS instead of the generator to ensure cost reduction (Moradi et al. 2017; Liu et al. 2020).

Additionally, Craparo et al. take a similar approach where a MILP optimization approach is developed to improve microgrid performance based on realistic weather data. Using the weather forecast data, Craparo et al. develop an optimal scheduling algorithm for hybrid microgrids which contain renewable power sources and conventional generators (Craparo et al. 2017). Bouaicha et al. use a similar optimization approach to improve microgrid performance using weather forecast data. Instead of optimizing over a specific weather data profile, Bouaicha et al. implement a planning approach that dynamically updates weather forecasts from historical data to create a rolling time horizon throughout the optimization (Bouaicha et al. 2020).

An another type of optimal energy management strategy is to employ the particle swarm optimization (PSO) approach. PSO is a swarm intelligence computation technique that allows

a controller to choose the most cost-effective way to deliver the power demand requirements based on the available power generating equipment within the microgrid architecture (del Valle et al. 2008; Li et al. 2017). When microgrids become very complex with many types of renewable power generators as well as ESSs, diesel generators, and the ability to connect to the main power grid, the integration of the swarm intelligence computation with an MILP approach results in an optimal solution with a shorter computation time when compared to a general MILP approach (Li et al. 2017). The swarm technique models the energy resources as individual particles that are parallel with each other. This makes each energy resource perform to the same rules outlined in the MILP. As each particle acts as a fully connected network of other entities, the particles find the best solution by gaining access to information of other energy resources within the network (del Valle et al. 2008). This is a parallel computational approach where all the energy resources are treated individually and can all run simultaneously to find the best solution while reducing computational run time (del Valle et al. 2008). Li et al. use the PSO optimization approach to reduce run time while discovering a scheduling algorithm that lowers energy production expense when compared to a non-PSO MILP-based approach (Li et al. 2017).

In general, researchers take the concept of optimal energy scheduling to a more sophisticated level by implementing algorithms, such as day-ahead scheduling technique where previous data is analyzed to predict the future power demand and the swarm technique where each energy source is treated independently. Energy scheduling is especially important when ESSs are introduced into the microgrid architecture as the system has the ability to store additional power for future use (Bahramirad et al. 2012; Chen et al. 2012). To reduce fuel cost and increase fuel efficiency, load scheduling becomes a crucial addition to the controller algorithm.

2.3 Fuel Consumption Minimization

The main goal in most stand-alone microgrid research is to minimize fuel consumption while maximizing generator efficiency. Hernandez-Aramburo et al. introduce a cost optimization scheme where several optimization models are developed to reduce generator fuel consumption while meeting the power demands. This particular study outlines four different power-sharing techniques to determine the optimal way to share the load between two gas-engine generators (Hernandez-Aramburo et al. 2005). Similar to optimal energy scheduling

studies and generator/energy storage sizing research, Hernandez-Aramburo et al. compare fuel consumption between the linear, nonlinear, dynamic, and optimal power sharing strategies to show that the optimal power sharing strategy on a highly nonlinear power sharing scheme maximizes financial benefits for a microgrid (Katiraei and Abbey 2007; Bahramirad et al. 2012; Moradi et al. 2017; Liu et al. 2020; Hernandez-Aramburo et al. 2005).

Kiser analyses the integration of ESS into an existing microgrid to assess fuel consumption on various power demand profiles obtained from U.S. military FOBs in the Middle East (Kiser 2018). Kiser explores the integration of various DoD technologies to determine their effect on generator fuel consumption. Kiser finds minimal change in fuel consumption when various technologies are analyzed with an integrated energy storage microgrid (Kiser 2018).

In addition to studies on microgrid architecture modification and energy management optimization techniques, Bhandari et al. introduce an approach where fuel consumption can be minimized using PV cells, batteries, and generator cycling. This study introduces several microgrid modifications with different size combinations of battery, generator, and PV cells to identify the optimal architecture by calculating the overall fuel consumption (Bhandari et al. 2013). As a result, Bhandari et al. conclude that a combination of a 30 kilowatt (kW) generator, battery, and a 30 kW PV unit results in the lowest overall cost of electricity and fuel consumption, but with the highest initial capital cost (Bhandari et al. 2013). In most microgrid optimization studies, the main goal is to minimize generator cumulative fuel consumption. As fuel consumption is one of the most important measures of performance identified in previous studies, the goal of this thesis is to minimize fuel consumption while ensuring that the power demand is efficiently met.

2.4 Fuel Efficiency with Fluctuating Loads

Fuel efficiency is an important generator characteristic that must be considered when fuel consumption is a microgrid's main performance measure. To include fuel efficiency into the notional generator, Hernandez-Aramburo et al. introduce a penalty term that is added to the cost function (Hernandez-Aramburo et al. 2005). A penalty is incorporated into the objective function when the generator operates outside the optimal operating region based on change in generator output between the present load and the previous load. This ensures that additional fuel consumption is accounted for when the generator power output fluctuates

in accordance with the power demand.

To reduce the effect of the generator penalty, Kiser integrates an ESS to help increase fuel efficiency during generator power output fluctuations (Kiser 2018). Kiser's optimization model uses the ESS to assist the generators when the change in load becomes large, which results in an overall long-run average of about 1.5% savings in fuel (Kiser 2018). Penalizing the generator by increasing fuel consumption is a more realistic approach when modeling generators that must meet fluctuating loads. From previous studies, a realistic approach to model a power system with fluctuating loads is to add a penalty term. The penalty term takes additional fuel consumption when generator power output varies at each time step. The addition of the ESS could result in a more fuel-efficient power system. The ESS offsets generator penalty costs caused by sudden changes in generator output based on fluctuating power demand.

CHAPTER 3:
Methodology

This chapter describes our MILP optimization model of an FOB microgrid, where the primary objective is to minimize the overall generator fuel consumption while satisfying a required power demand. Our microgrid equipment consists of a fuel-based generator and an ESS, and we exercise our model using power demand data collected from a U.S. FOB located in the Middle East.

The MILP acts as a rudimentary power system controller which controls the power flow between the generator and ESS to satisfy the demand. Figure 3.1 depicts our controller architecture, including the power flow and communication flow. The controller maintains communication between the three separate components; however, power is only produced by the generator. This power may satisfy the demand directly, or supplementary generator output power charges the ESS, while the ESS may discharge power to meet demand.

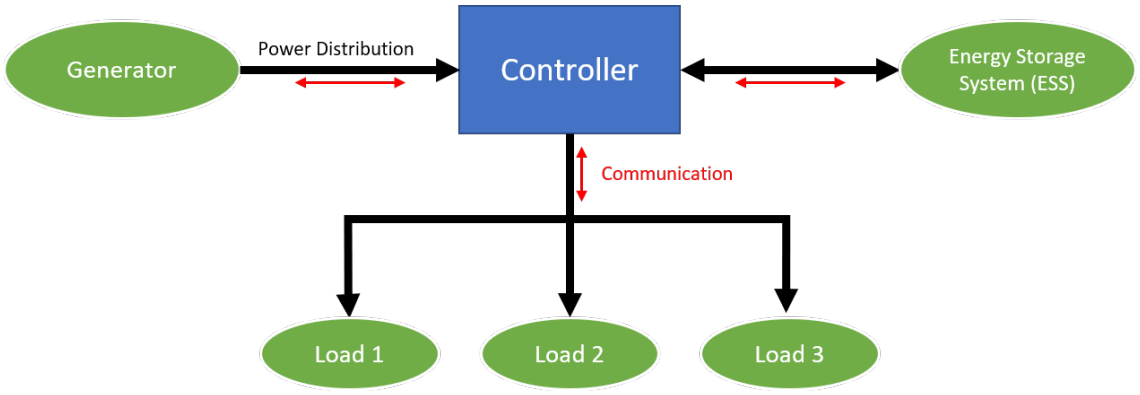

Figure 3.1. Notional microgrid controller flowchart with power distribution and communication flow. Adapted from Craparo and Sprague (2019).

3.1 Microgrid Architecture

This section describes the major components that make up a typical FOB microgrid in the Middle East.

3.1.1 Fuel-Based Generator

We model a 60 kW, 60 hertz (Hz) Advanced Medium Mobile Power Sources (AMMPS) generator. This is a U.S. Army-authorized power-generating unit that replaces the second generation Tactical Quiet Generator (TQG). The generator upgrade significantly decreases logistic footprint while improving fuel consumption as well as reducing noise and weight (United States Army Acquisition Support Center 2017). We model generator fuel consumption using a linear approximation based on the steady-state consumption data depicted in Figure 3.2 obtained from U.S. Army Base Camp Integration Lab (Singleton 2017).

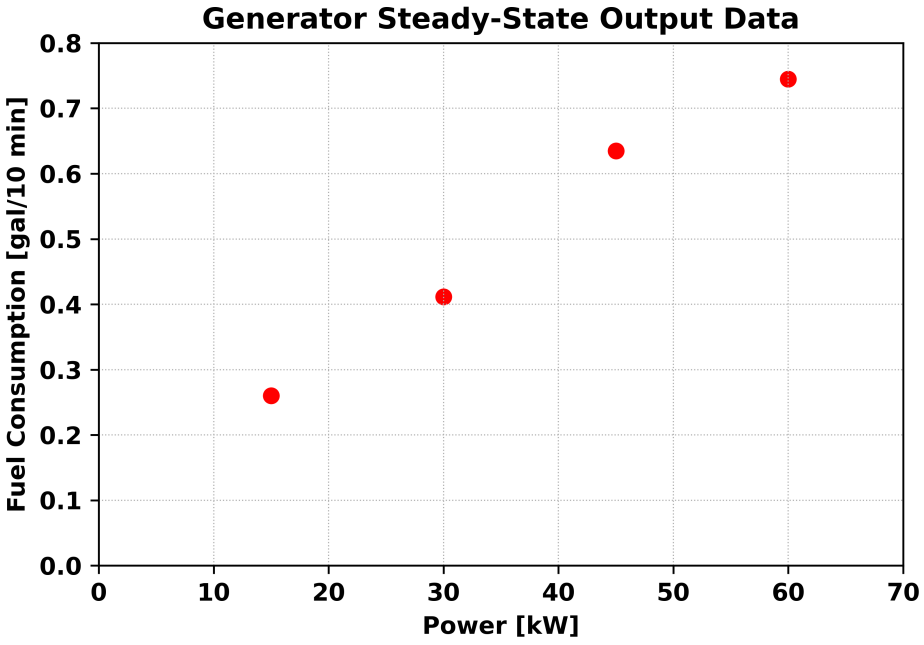

Figure 3.2. 60 kW AMMPS generator steady-state fuel consumption data at four distinct operating regions obtained from previous studies. Adapted from Singleton (2017).

We restrict our generator to operate between a minimum power output of 15 kW and a maximum power output of 60 kW.

3.1.2 Energy Storage System

We model a 25 kilowatt-hours (kWh) ESS with a maximum rate of charge and discharge rate of 20 kW and a 90% round trip efficiency (RTE) based on the previous literature review discussed in Chapter 2; these values approximate the characteristics of a lithium-ion battery. Most lithium-ion batteries have an RTE between 90% and 95% (Li and Tseng 2015). We constrain the ESS to maintain a state of charge (SOC) between 20% to 80% in order to prolong the lifespan of the ESS (Moseley and Garche 2015; Majima et al. 2001). We initialize the ESS to an SOC of 50% in the first time period to simulate a continuously operating power system.

3.2 Optimization Model

The overall objective of the MILP optimization model is to minimize generator fuel consumption while satisfying demand $demand_t$ in each time period t in T. Demand may be satisfied by the generator, the ESS, or some combination of the two. Additionally, the generator can produce power exceeding the demand request, and the additional power charges the ESS. We denote the power produced by the generator in time step t as gen_t, the power used to charge the ESS (battery) as $cbatt_t$, and the power discharged from the battery as $dbatt_t$. Then, the power balance equation is

$$demand_t = gen_t + effd \cdot dbatt_t - cbatt_t \quad \forall\, t \in T$$

where *effd* is the discharge efficiency of the battery. We express the battery SOC soc_t as a percentage of the maximum charge $battcap$ and calculate it as

$$soc_t = soc_{t-1} - dbatt_t \cdot \frac{dt}{battcap} + effc \cdot cbatt_t \cdot \frac{dt}{battcap} \quad \forall\, t \in T$$

where *effc* represents the charging efficiency of the battery and dt represents the length of our time step in hours.

To model the physical limitations of the generator, we define $minGen$ and $maxGen$ as the generator's minimum and maximum power output, respectively:

$$minGen \leq gen_t \leq maxGen \quad \forall\, t \in T.$$

Figure 3.2 depicts the generator fuel consumption between the minimum and maximum power output based on collected fuel consumption coefficients specific to the respective generator. Similarly, we define $maxCharge$ and $maxDischarge$ as the maximum charge and discharge rates of the battery, and we constrain the battery to maintain an SOC between $minSOC$ and $maxSOC$:

$$0 \leq dbatt_t \leq maxDischarge \quad \forall\, t \in T$$

$$0 \leq cbatt_t \leq maxCharge \quad \forall\, t \in T$$

$$minSOC \leq soc_t \leq maxSOC \quad \forall\, t \in T.$$

To simulate ongoing operations and avoid end-of-horizon effects, we require that the final SOC equal the initial SOC:

$$soc_1 = soc_{|T|}.$$

The overall objective of the MILP optimization model is to minimize the fuel consumed by the generator. As shown in Figure 3.3, we use a linear fit to represent the fuel consumption based on a steady-state load. This steady-state fuel consumption is typically the only fuel consumption term accounted for in previous studies. The objective function in Equation 3.1 is defined by the slope and intercept where sl^b is the fuel consumption slope of 0.0113 and in^b is the fuel consumption intercept of 0.0933.

$$\min \sum_{t \in T} \left[sl^b gen_t + in^b + penalty_t \right] \tag{3.1}$$

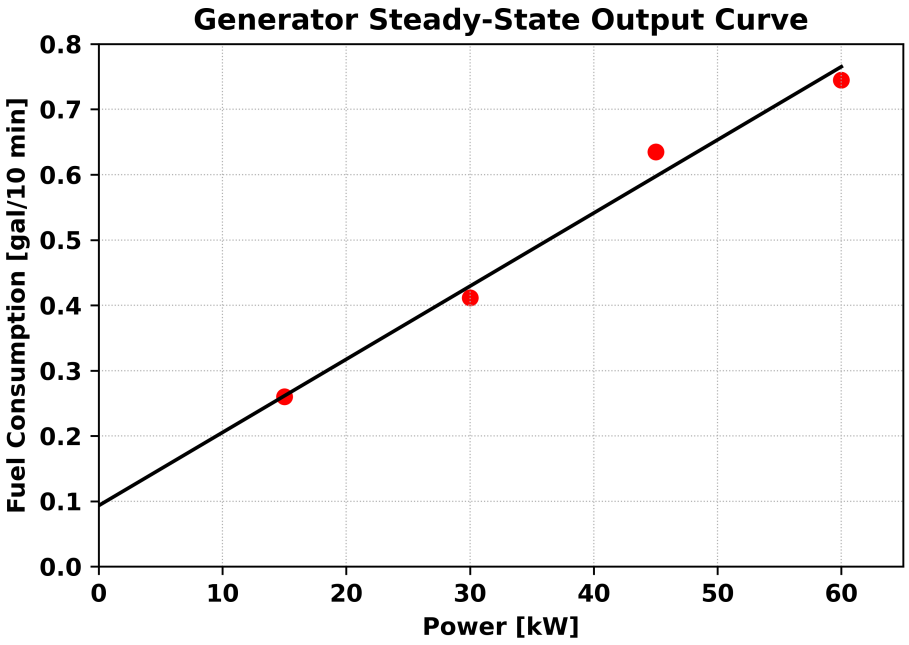

Figure 3.3. 60 kW AMMPS generator fuel consumption with a linear fit based on generator steady-state power output data. Adapted from Singleton (2017).

The fuel consumption shown in Figure 3.3 depicts a perfect linear curve based on the generator power output. Figure 3.4 shows the corresponding generator fuel efficiency curve. The fuel efficiency increases as more power is produced by the generator.

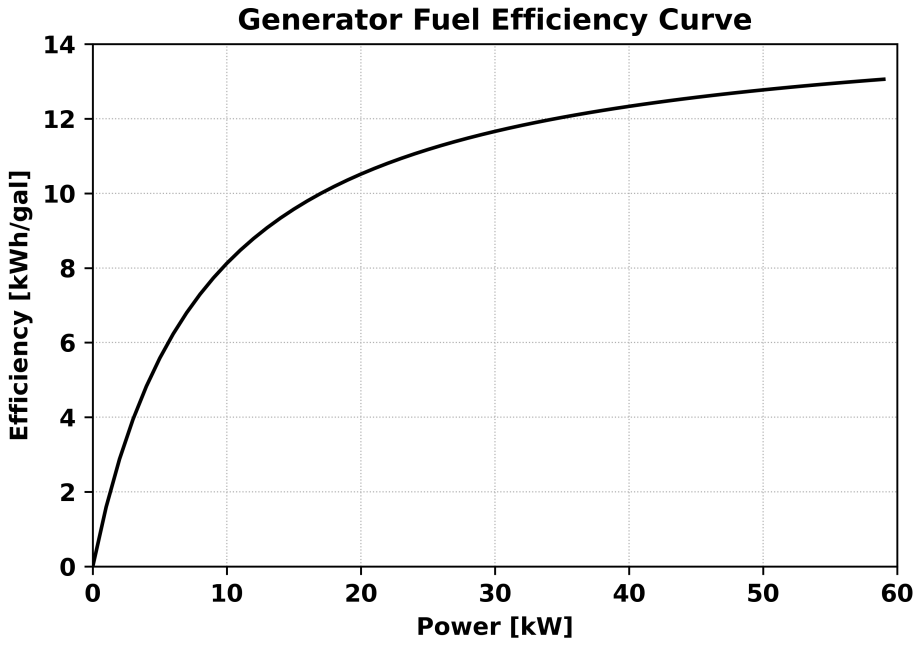

Figure 3.4. 60 kW AMMPS generator fuel efficiency curve based on generator steady-state power output data. Adapted from Singleton (2017).

To address our primary study objective, we include an additional "penalty term" $penalty_t$ to capture the efficiency loss incurred when the generator output power fluctuates rapidly from time period to time period:

$$\min \sum_{t \in T} \left[sl^b gen_t + in^b + penalty_t \right]. \tag{3.2}$$

We now describe our methodology for calculating $penalty_t$.

3.3 Generator Penalty Concept

We explore and develop three different approaches to calculate the "penalty term" $penalty_t$ in Equation 3.2. As a base case, we consider $penalty_t = 0$ for all t in T (no generator efficiency loss during load fluctuation), which is the approach typically taken in previous studies. Next, we calculate $penalty_t$ as a linear function of the percentage change in generator output from time period to time period. Finally, we calculate $penalty_t$ as a piecewise linear

function of the percentage change in generator output.

3.3.1 No Penalty Approach

As a base case, we first set $penalty_t = 0$ for all t in T. This allows us to compare the policies resulting from standard modeling approaches to those that consider a loss of generator efficiency when loads fluctuate rapidly. The objective function without the penalty term is

$$\min \sum_{t \in T} \left[sl^b gen_t + in^b \right]$$

where the linear fit curve, itself, represents the fuel consumption.

3.3.2 Linear Penalty Approach

Next, we express $penalty_t$ as a linear function of the percentage change in generator output from one time period to the next. Let $frac\_chg_t$ denote the fractional change in generator output from time period $t-1$ to time period t. Then, $frac\_chg_t$ is exactly calculated as

$$frac\_chg_t = \frac{|gen_t - gen_{t-1}|}{gen_{t-1}} \quad \forall\, t \in T. \tag{3.3}$$

In order to formulate a linear optimization model, we instead calculate an approximate value for $frac\_chg_t$. First, we calculate the absolute change in generator output $abs\_chg_t = |gen_t - gen_{t-1}|$ for all t in T using the linear constraints

$$abs\_chg_1 = 0$$

$$gen_t - gen_{t-1} \leq abs\_chg_t \quad \forall\, t \in [2, ..., T] \tag{3.4}$$

$$gen_{t-1} - gen_t \leq abs\_chg_t \quad \forall\, t \in [2, ..., T] \tag{3.5}$$

where we rely on the fact that fluctuations are penalized in our objective function, and thus the solver chooses the smallest feasible value for abs_chg_t, given the values of gen_{t-1} and gen_t.

After calculating the value of abs_chg_t using Equations 3.4 and 3.5, we must address the non-linearity caused by the gen_{t-1} term in the denominator of Equation 3.3. We do this by partitioning the generator's operating range $[minGen, maxGen]$ into a set of discrete operating regions $i \in I$. Each operating region i is defined by its lower bound l_i and upper bound u_i, where $l_1 = minGen$, $u_{|I|} = maxGen$, and $l_i = u_{i-1}$ for $i = 2, ..., |I|$. We utilize binary variable $Y_{i,t}$ to indicate that the generator is operating in region i at time t and enforce this using the following constraints:

$$\sum_{i \in I} Y_{i,t} l_i \leq gen_t \leq \sum_{i \in I} Y_{i,t} u_i \quad \forall\, t \in T$$

$$\sum_{i \in I} Y_{i,t} = 1 \quad \forall\, t \in T.$$

To obtain our linear approximation to Equation 3.3, we replace the gen_{t-1} term in the denominator by the midpoint of the generator's operating region at time $t-1$, i.e., $\sum_{i \in I} Y_{i,t-1} \frac{l_i + u_i}{2}$. This yields the following expression for $frac\_chg_t$:

$$frac\_chg_t = \sum_{i \in I} \frac{Y_{i,t-1} abs\_chg_t}{(l_i + u_i)/2} \quad \forall\, t \in T,$$

which is still nonlinear due to the product of a binary variable and a continuous variable in the numerator. However, we linearize this expression by defining the continuous variable $P_{i,t}$ and using the following system of constraints to ensure that $P_{i,t} = Y_{i,t-1} abs\_chg_t$:

$$0 \leq P_{i,t} \leq Y_{i,t-1}(maxGen - minGen) \quad \forall\, i \in I,\ t \in T$$

$$abs\_chg_t - (maxGen - minGen)\big(1 - Y_{i,t-1}\big) \leq P_{i,t} \leq abs\_chg_t \quad \forall\, i \in I,\ t \in T.$$

Our expression for $frac\_chg_t$ is then

$$frac\_chg_t = \sum_{i \in I} \frac{P_{i,t}}{(l_i + u_i)/2} \quad \forall\, t \in T.$$

Lastly, we define scalar penalty coefficient $pcoe$ and express our objective function with

linear fluctuation penalty as

$$\min \sum_{t \in T} \left[sl^b gen_t + in^b + pcoe \sum_{i \in I} \frac{2P_{i,t}}{l_i + u_i} \right].$$

3.3.3 Piecewise Linear Penalty Approach

Finally, we expand upon our linear penalty approach by constructing a piecewise linear penalty term. This allows us to model more complex penalty functions, such as a marginal penalty that increases with the fractional change in generator output $frac\_chg_t$. To construct our piecewise linear function, we first define a discrete set of regions for the value of $frac\_chg_t$ for all t in T, defined similarly to the generator operating regions in Section 3.3.2. Denote the lower and upper bounds for fractional change region $h \in H$ as lo_h and up_h, where $lo_1 = 0$, $up_{|H|} = \frac{maxGen - minGen}{(l_1 + u_1)/2}$, and $lo_h = up_{h-1}$ for $h = 2, ..., |H|$. Then, let binary variable $W_{h,t}$ indicate that $frac\_chg_t$ lies within region h, and enforce this using the following constraints:

$$\sum_{h \in H} W_{h,t} lo_h \leq frac\_chg_t \leq \sum_{h \in H} W_{h,t} up_h \quad \forall\, t \in T$$

$$\sum_{h \in H} W_{h,t} = 1 \quad \forall\, t \in T.$$

Let slo_h and int_h denote the slope and intercept, respectively, of the piecewise linear penalty function in region h. Then, we wish to express $penalty_t$ as

$$penalty_t = \sum_{h \in H} W_{h,t} \left(slo_h frac\_chg_t + int_h \right) \quad \forall\, h \in H,\ t \in T$$

where, again, we have a product of a binary variable and a continuous variable $W_{h,t} frac\_chg_t$. To linearize this term, we introduce the continuous decision variable $Q_{h,t}$ and use the following system of constraints to ensure that $Q_{h,t} = W_{h,t} frac\_chg_t$:

$$0 \leq Q_{h,t} \leq up_{|H|} W_{h,t} \quad \forall\, h \in H,\ t \in T$$

$$frac\_chg_t - up_{|H|}\left(1 - W_{h,t}\right) \leq Q_{h,t} \leq frac\_chg_t \quad \forall\, h \in H,\ t \in T.$$

Thus, our objective function is

$$\min \sum_{t \in T} \left[sl^b gen_t + in^b + \sum_{h \in H} \left(slo_h Q_{h,t} + int_h W_{h,t} \right) \right].$$

Our model appears in its entirety in Appendix A.1.

We experiment with four different piecewise linear penalties shown in Figure 3.5. We calculate $slo_h = h \cdot slo_1$ for each linearization region $h = 1, ..., |H|$. The intercept int_h of each segment in the piecewise linear curve is calculated so as to sustain a continuous piecewise linear function. The four piecewise linear functions are defined by their initial slopes (i.e., slo_1), which vary from 0.1 to 0.4 as shown in the figure legend, with $int_1 = 0$ for each function.

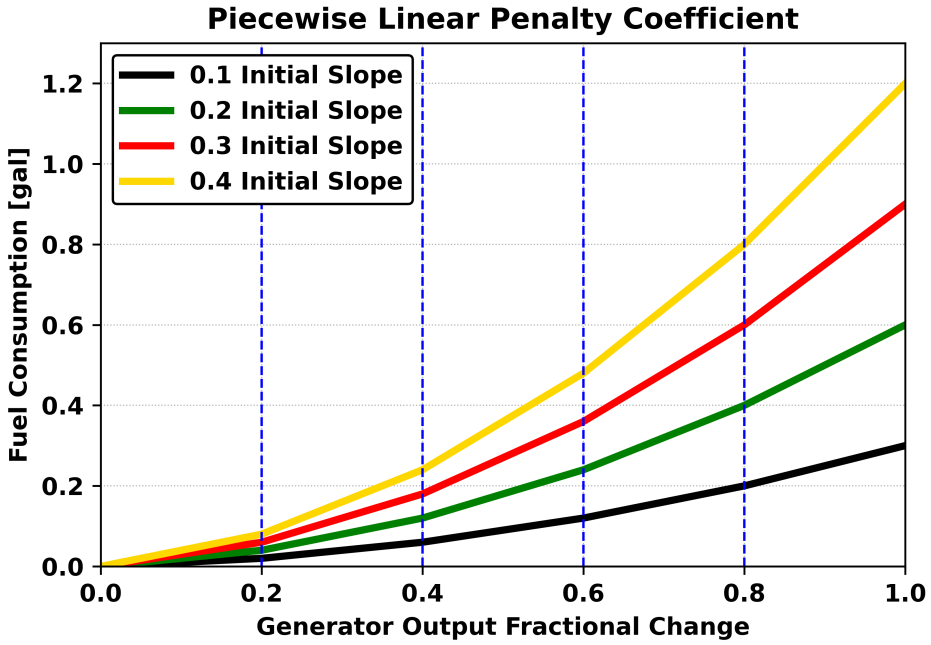

Figure 3.5. Fuel consumption plots for piecewise linear penalty profiles with varying initial slopes.

CHAPTER 4:
Results and Analysis

We now exercise the optimization model described in Chapter 3 on several scenarios. We consider three demand scenarios: a simple notional demand profile, and two demand profiles based on historical data, one from the winter season and one from the summer season. For each demand profile, we first study the impact of including an ESS in our microgrid architecture by solving the model with and without an ESS, then we quantify the impact that various penalty terms have on the microgrid's fuel consumption and the optimal generator and ESS usage.

We implement our model using Python's Pyomo package and solve it using the IBM ILOG CPLEX Interactive Optimizer 12.10.0.0 on a computer with 16 GB RAM and a 2.60 GHz CPU (International Business Machines Corporation (IBM) 2009). The instances described in this chapter contain approximately 414–9501 constraints and 221–5761 decision variables, of which 60–2016 are binary. These instances solve to a 0–1% optimality gap in approximately 1–20 seconds.

4.1 Notional Power Demand Case Study

Figure 4.1 shows a 200-minutes (min) notional power demand profile with a 10-min time step. This profile is developed to resemble realistic loads with a combination of large steps and constant power consumption. Since the generator is rated at 60 kW, the notional demand profile is designed to stay within the 60 kW power output range. We first compare results obtained with and without the ESS to highlight the impact of microgrid ESS integration. Then, with this baseline understanding of the performance difference between the model with and without ESS, we impose a penalty on the generator to model the loss of efficiency incurred when the generator load fluctuates.

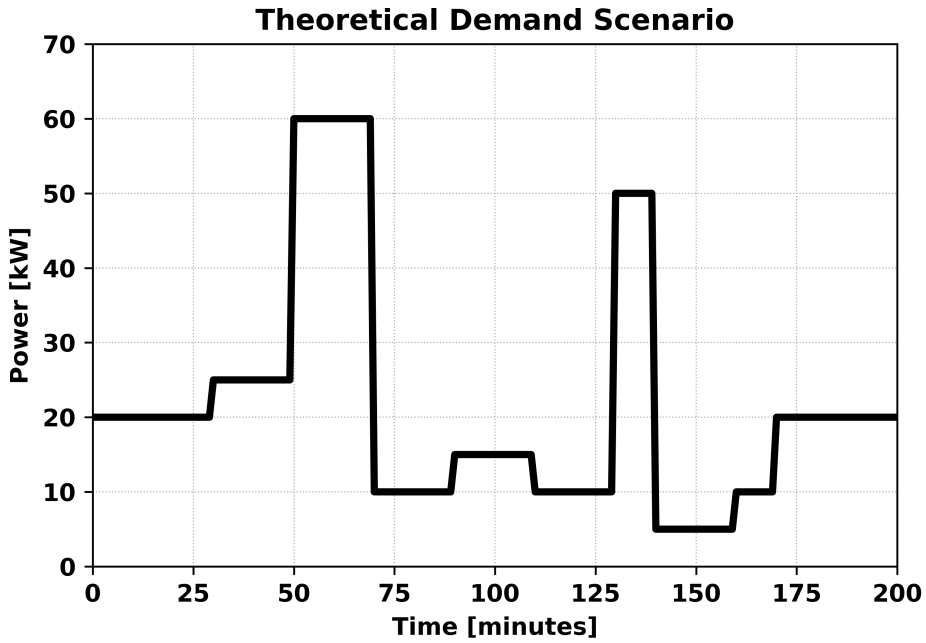

Figure 4.1. Theoretical demand profile over a 200-min horizon with 10-min intervals designed for a 60 kW generator.

4.1.1 Optimization With and Without ESS

We determine the impact of integrating the ESS into the microgrid by comparing the results obtained without ESS and with ESS for a theoretical demand profile depicted in Figure 4.1. The optimal solution is shown in Figure 4.2, where the power produced by the generator is depicted in green along with the theoretical demand profile (black solid line). The dark green in Figure 4.2a represents the generator power output at each time step t that is used to satisfy demand, outlined in black. The light green color shows the generator output power that exceeds the required demand at that respective time step t. This occurs because the generator has a 15 kW minimum power output threshold. Excess power is produced when the demand is less than 15 kW, and in practical applications, this excess may be stored if possible. The maximum generator output power is set at 60 kW. The cumulative fuel consumption in each time step t is shown in Figure 4.2b. The generator consumes a total of 7.19 gallons (gal) of fuel, and 79.17 kWh of cumulative energy is produced at the end of the 200-min time horizon when solved to a 0% optimality gap.

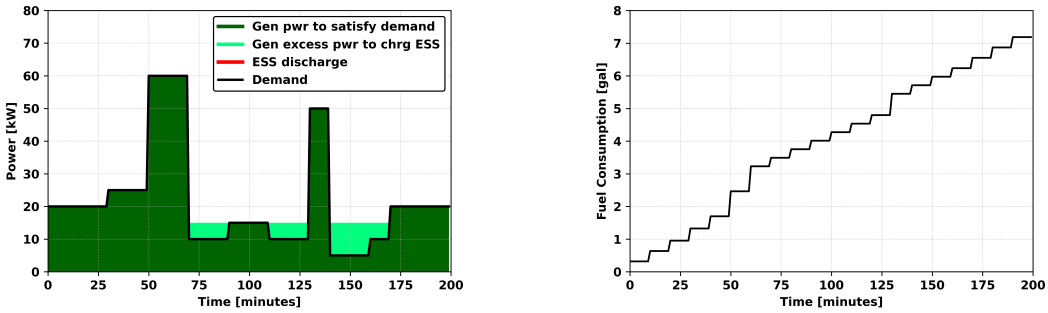

(a) Power output plot

(b) Generator fuel consumption plot

Figure 4.2. Power output and fuel consumption for architecture without ESS

Next, we introduce an ESS to our microgrid with the goal of determining whether the ESS improves the performance of the microgrid power system by decreasing fuel consumption. Figure 4.3a shows the optimal solution for the microgrid with ESS. In this solution, the generator supplies 89.42% of the demand and the ESS supplies the remaining 10.58% of the demand. The overall fuel consumption decreases to 6.68 gal when the ESS is integrated into the architecture. With approximately a 37% difference in cumulative fuel consumption, the generator in the optimization model with ESS produces a total of 71.58 kWh. Figure 4.3b shows the SOC of the ESS. This figure confirms that the ESS discharges energy to satisfy the power demand during sudden load step increases and then it is charged when the power demand falls below 15 kW. Based on the initial SOC of 50%, the ESS, on average, sustains an SOC of 40% with a minimum SOC of 25.05% and a maximum SOC of 50%.

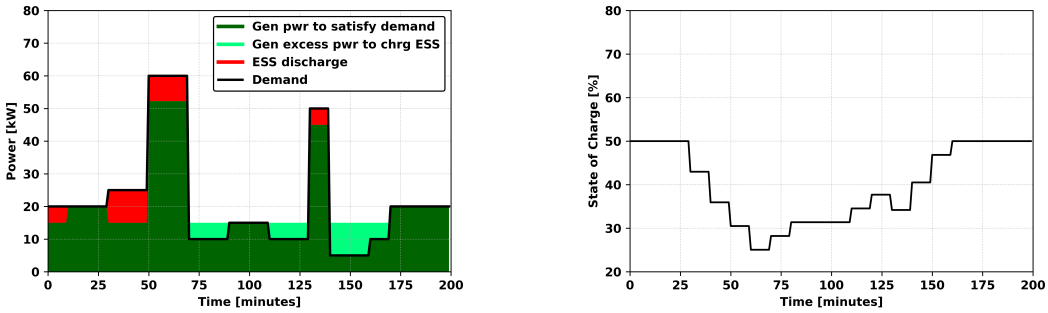

(a) Power production plot

(b) ESS SOC plot

Figure 4.3. Power output and SOC plot for architecture with ESS

The results shown in Figure 4.3 demonstrate that the optimal solution utilizes the ESS to assist in satisfying larger power demand fluctuations and decrease fuel consumption. This phenomenon is apparent in Figure 4.3a around 50 min and 70 min, where the power demand profile presents the largest steps and the ESS is utilized to satisfy these increased demands. However, with no penalty on generator fluctuations, we also see the ESS being utilized to satisfy relatively stable demands. This is apparent around 0–50 min, where the generator output actually fluctuates more than the demand itself.

4.1.2 Linear Penalty

In our notional example, the ESS allows a 37% reduction in fuel consumption compared to the case without ESS. However, as we have seen, this fuel savings may come at the cost of additional generator output fluctuations. Realistically, a sudden change in generator output power causes additional stress on the generator, decreasing its operational lifetime. We also expect such fluctuations to decrease fuel efficiency, although to our knowledge no studies have attempted to measure this empirically. To study the impact of this loss of efficiency, we now introduce a linear penalty term on the generator output power fluctuation. Table 4.1 summarizes the optimal fuel consumption and breakdown of power production in the optimal solution for linear penalty coefficient values of 0.2 gal/Δ, 0.4 gal/Δ, 0.6 gal/Δ, and 0.8 gal/Δ, where Δ is the linear approximation of the percentage change in generator output from one time step to the next, as described in Chapter 3.

Table 4.1. Optimal fuel consumption and power output with linear penalty.

Penalty	**Cumulative Fuel Consumption [gal]**	**Demand met by Generator [%]**	**Demand met by ESS [%]**	**Generator output used to charge ESS [%]**
No Penalty	6.68	89.42	10.58	10.47
Linear 0.2	7.19	79.96	20.04	20.97
Linear 0.4	7.63	80.80	19.20	20.97
Linear 0.6	8.06	80.80	19.20	20.97
Linear 0.8	8.49	80.80	19.20	20.97

Table 4.1 shows that fuel consumption increases significantly when generator efficiency loss is implemented by imposing a penalty. The results indicate the importance of taking the generator efficiency loss into account when computing the cumulative fuel consumption. The trend in Table 4.1 shows an increase in fuel consumption when a more significant penalty is imposed on the generator. For each value of the linear penalty coefficient, the generator satisfies approximately 80% of the load while the ESS satisfies approximately 20% of the load. This is significantly different from the case with no penalty, where the generator satisfies nearly 90% of the demand. The optimal power production between the generator and the ESS changes minimally across the four varying penalty scenarios; however, as expected, fuel consumption increases as the weight of the penalty becomes greater.

4.1.3 Piecewise Linear Penalty

We now consider piecewise linear penalty functions, as shown in Figure 3.5. Table 4.2 shows the optimization model results when the piecewise linear penalty initial slopes of 0.1 gal/Δ, 0.2 gal/Δ, 0.3 gal/Δ, and 0.4 gal/Δ are added to the base fuel consumption calculation at each time step t.

Table 4.2. Optimal fuel consumption and power output with piecewise linear penalty.

Penalty	Cumulative Fuel Consumption [gal]	Demand met by Generator [%]	Demand met by ESS [%]	Generator output used to charge ESS [%]
No Penalty	6.68	89.42	10.58	10.47
Pi. Lin. 0.1	6.98	79.96	20.04	20.97
Pi. Lin. 0.2	7.23	79.96	20.04	20.97
Pi. Lin. 0.3	7.47	80.51	19.49	20.97
Pi. Lin. 0.4	7.71	80.51	19.49	20.97

Table 4.2 reveals an increase in cumulative fuel consumption as a larger penalty coefficient is added to the base fuel consumption calculation. As with the linear penalty results shown in Table 4.1, we see a substantial difference in optimal power production between the base case with no penalty and the cases with a penalty, but little difference between the various penalty cases. Again, our numerical results indicate that the slope variation in the four different penalty cases is insignificant; however, taking into account for the generator efficiency loss is a vital aspect to the fuel consumption calculation.

4.2 Winter Power Demand Case Study

Having gained some initial insights from our simple demand scenario, we now consider more realistic scenarios derived from several power demand profiles from a U.S. FOB located in the Middle East collected by the Army Logistics Innovation Agency (LIA) during the Contingency Base – Demand Data Collection (CB-DDC) project. Figure 4.4 shows our first power demand input, which we create based on FOB demand during a 48-hour period in the winter season.

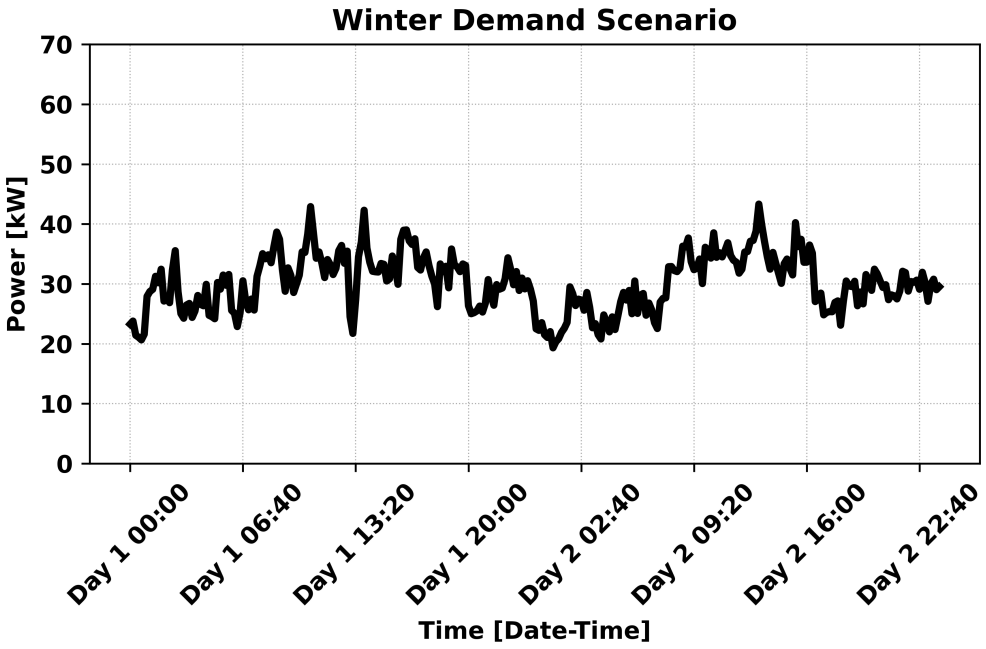

Figure 4.4. U.S. FOB power demand scenario over a 48-hour time frame during the winter season.

4.2.1 Optimization With and Without ESS

We first compare the optimal power flow without ESS and with ESS, with no penalty term. Figure 4.5 shows the optimal generator power output without ESS (Figure 4.5a) and with ESS (Figure 4.5b). In both architecture configurations, the generator supplies most of the load throughout the 48-hour scenario, as shown in the dark green shaded region and summarized numerically in Table 4.3. Notably, as in the preliminary demand scenario, the presence of an ESS with no penalty results in more generator output fluctuation than is necessary to satisfy demand.

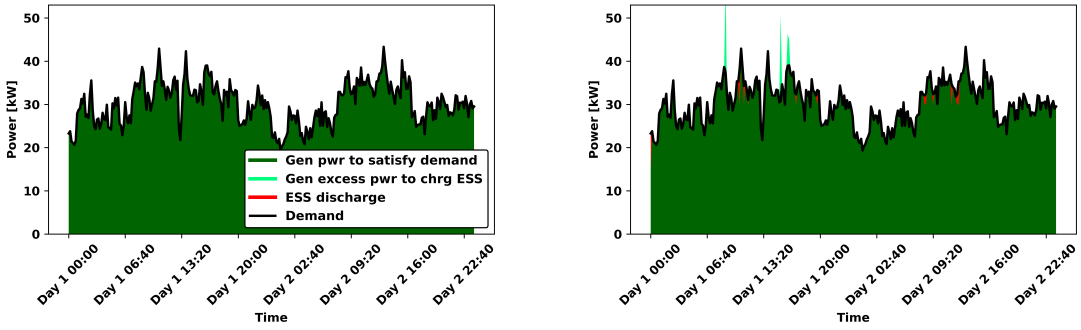

(a) Architecture without ESS

(b) Architecture with ESS

Figure 4.5. Power output plot for winter demand without ESS (left) and with ESS (right).

Table 4.3. Optimal fuel consumption and power output for the winter demand scenario with and without ESS.

Architecture	**Cumulative Fuel Consumption [gal]**	**Demand met by Generator [%]**	**Demand met by ESS [%]**	**Generator output used to charge ESS [%]**
Without ESS	124.19	100	0	0
With ESS	124.15	99.35	0.65	0.70

4.2.2 Linear Penalty

We now impose a linear penalty on generator output fluctuations. Figure 4.6 shows the power production breakdown between the generator and the ESS for linear penalty coefficients of 0.2 gal/Δ, 0.4 gal/Δ, 0.6 gal/Δ, and 0.8 gal/Δ, and Table 4.4 summarizes these results numerically. These instances are solved to a 1% optimality gap.

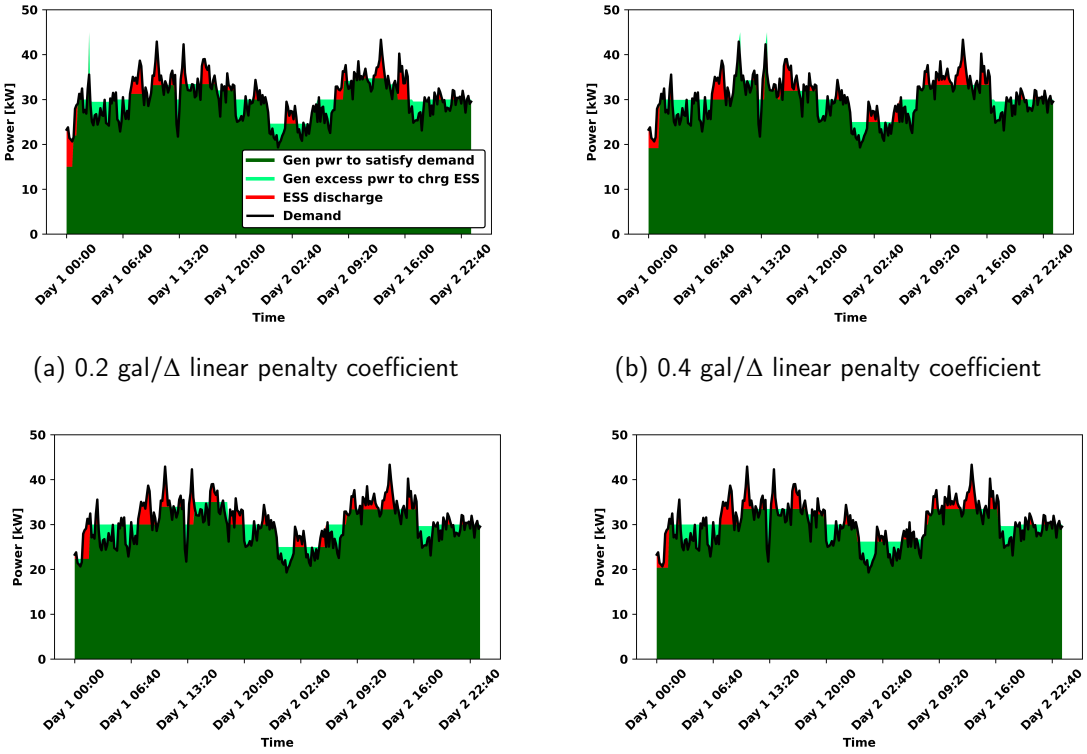

(a) 0.2 gal/Δ linear penalty coefficient

(b) 0.4 gal/Δ linear penalty coefficient

(c) 0.6 gal/Δ linear penalty coefficient

(d) 0.8 gal/Δ linear penalty coefficient

Figure 4.6. Power output for the winter demand scenario with linear penalties.

As with the preliminary demand scenario, we observe a significant qualitative change in the optimal generator output profile relative to the case with no penalty, as well as a substantial increase in ESS utilization (though the ESS still satisfies only a small percentage of the overall demand). The optimal strategies that are graphically depicted in Figure 4.6 use the ESS when the power system experiences large demand spikes to prevent unnecessary generator fluctuation. The excess generator power output charges the ESS during time steps with less demand to ensure that enough charge is available for future demands.

Table 4.4. Optimal fuel consumption and power output with various linear penalties for the winter demand scenario.

Penalty	**Cumulative Fuel Consumption [gal]**	**Demand met by Generator [%]**	**Demand met by ESS [%]**	**Generator output used to charge ESS [%]**
No Penalty	124.15	99.35	0.65	0.70
Linear 0.2	125.17	95.95	4.05	4.40
Linear 0.4	125.60	95.98	4.02	4.42
Linear 0.6	125.46	95.75	4.26	4.72
Linear 0.8	125.46	96.00	4.00	4.41

4.2.3 Piecewise Linear Penalty

We now consider a piecewise linear penalty term, again using the four piecewise functions shown in Figure 3.5. Figure 4.7 displays our optimal solutions for these four scenarios (again solved to a 1% optimality gap), while Table 4.5 summarizes our results numerically.

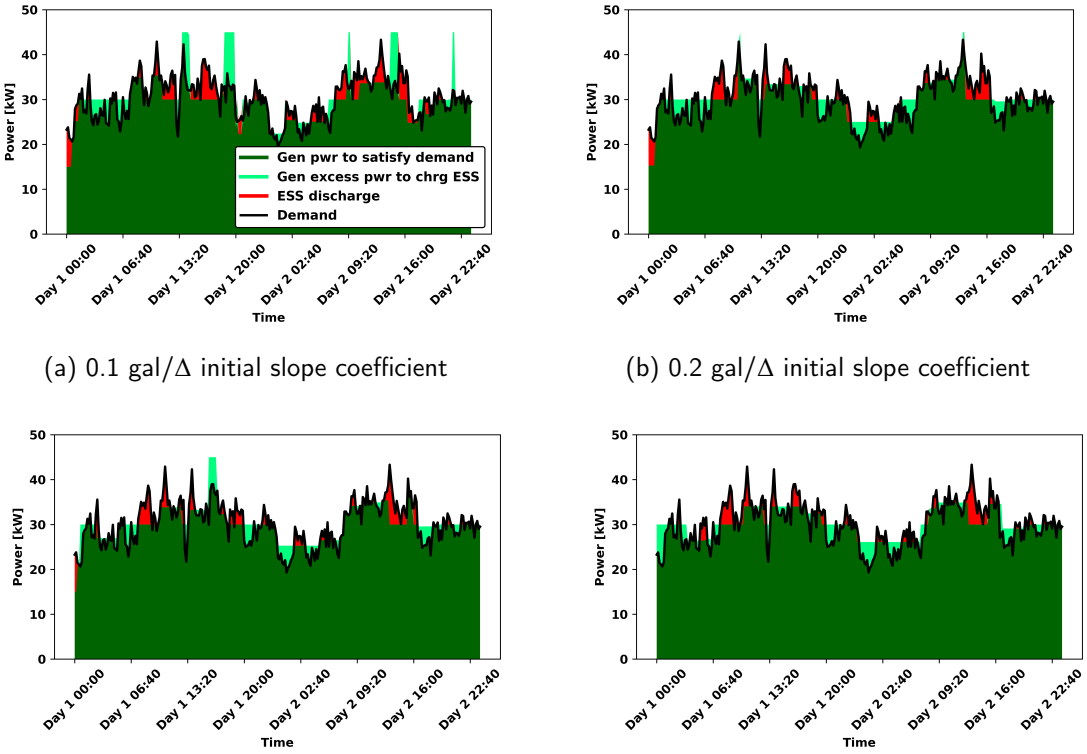

(a) 0.1 gal/Δ initial slope coefficient

(b) 0.2 gal/Δ initial slope coefficient

(c) 0.3 gal/Δ initial slope coefficient

(d) 0.4 gal/Δ initial slope coefficient

Figure 4.7. Power output plot based on piecewise linear penalties imposed on the generator for the winter demand scenario.

As before, we see that most of the demand is satisfied by the generator, as the dark green color dominates the surface area of the four power output plots. The additional power produced by the generator decreases slightly as the initial penalty slope increases, though the magnitude of the increase is insignificant in light of the 1% optimality gap. Qualitatively, a larger penalty imposed on the generator forces a more constant level of power production from the generator. As before, the ESS satisfies temporary demand spikes, while the generator produces excess power to charge the ESS during periods of low demand.

Table 4.5. Optimal fuel consumption and power output with various piecewise linear penalties for the winter demand scenario.

Penalty	**Cumulative Fuel Consumption [gal]**	**Demand met by Generator [%]**	**Demand met by ESS [%]**	**Generator output used to charge ESS [%]**
No Penalty	124.15	99.35	0.65	0.70
Pi. Lin. 0.1	125.49	94.54	5.46	6.01
Pi. Lin. 0.2	125.09	95.76	4.24	4.61
Pi. Lin. 0.3	125.54	95.96	4.04	4.39
Pi. Lin. 0.4	125.54	95.91	4.09	4.80

We again note that the presence of a penalty term significantly impacts both the optimal generator output profile and the percentage of demand satisfied by the generator and ESS, but the optimal solution does not vary significantly for the penalty values we consider.

Figure 4.8 again underscores the importance of imposing a penalty on the generator. The addition of the linear and piecewise linear penalty creates a drastic change in the optimal generator output. Indeed, for the excursion with an ESS and no penalty, we observe the generator output fluctuating *more* than the demand. The figure directly shows that the ESS is utilized more when the optimization includes generator efficiency loss. With the penalty imposed on the generator, the power distribution between the generator and the ESS significantly changes, as the ESS takes over satisfying time-varying, peak demands and the generator outputs constant power.

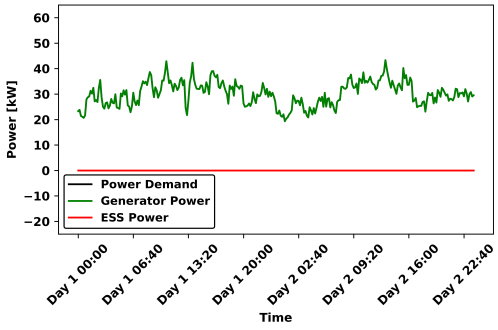

(a) No ESS & No penalty

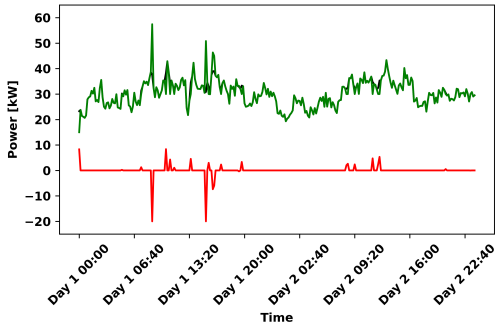

(b) No penalty

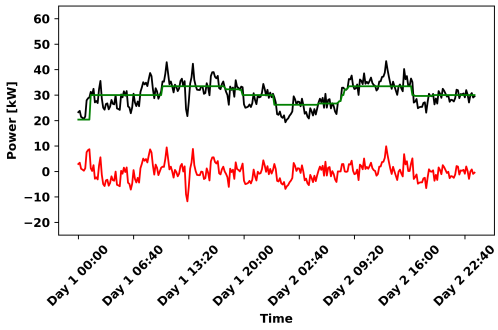

(c) 0.8 gal/Δ linear penalty coefficient

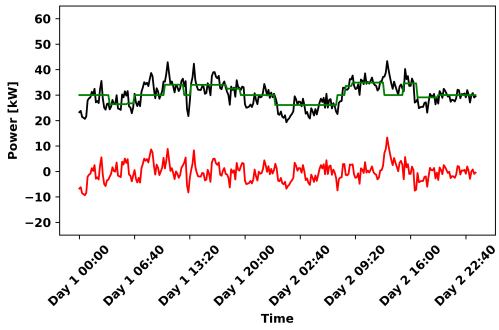

(d) 0.4 gal/Δ initial slope piecewise linear coefficient

Figure 4.8. Optimal power distribution over various architectures for the winter demand scenario.

4.3 Summer Power Demand Case Study

We now consider demand data obtained during the summer months from a U.S. FOB located in the Middle East collected by the Army LIA during the CB-DDC project. The overall power demand increases on average 15–20 kW compared to the winter power demand profile. We wish to determine whether a higher average power demand alters the optimal power production between the generator and ESS during a 48-hour optimization scenario. Figure 4.9 depicts the power demand profile in a 48-hour period, which we implement in the optimization model.

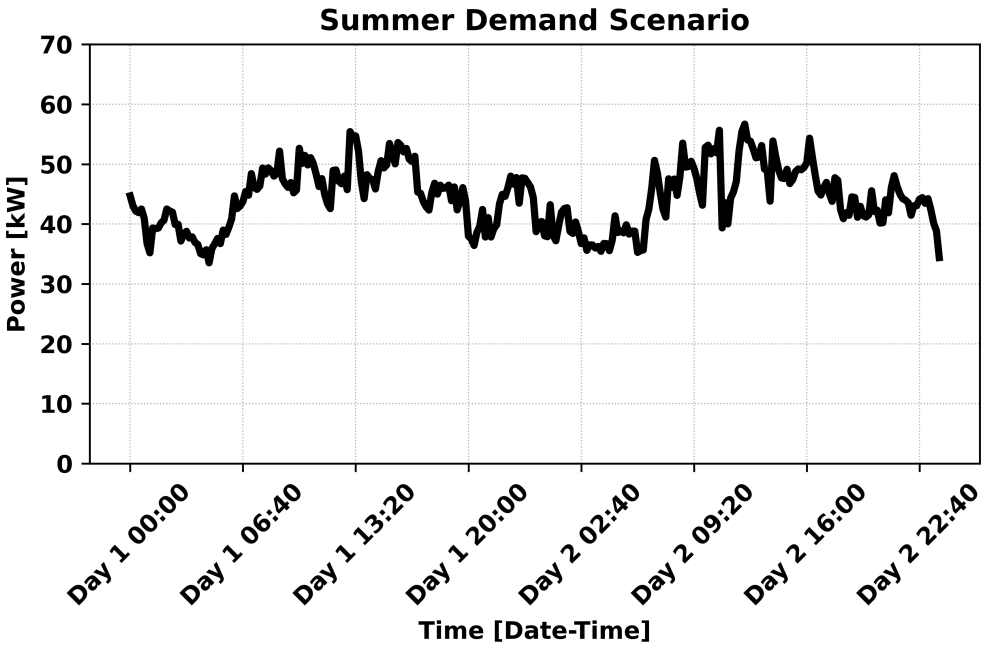

Figure 4.9. U.S. FOB power demand scenario over a 48-hour time frame during the summer season.

4.3.1 Optimization With and Without ESS

As before, we first compare the optimal power flow with ESS and without ESS; these results appear in Figure 4.10 and are summarized numerically in Table 4.6. In both architecture configurations, the generator supplies most of the load throughout the 48-hour demand scenario. As we observed in the winter demand scenario, the presence of an ESS results in increased generator output fluctuations when these fluctuations are not penalized. In contrast to the winter demand scenario, we now observe the ESS satisfying a larger portion of the demand, although the generator still satisfies the majority of the demand.

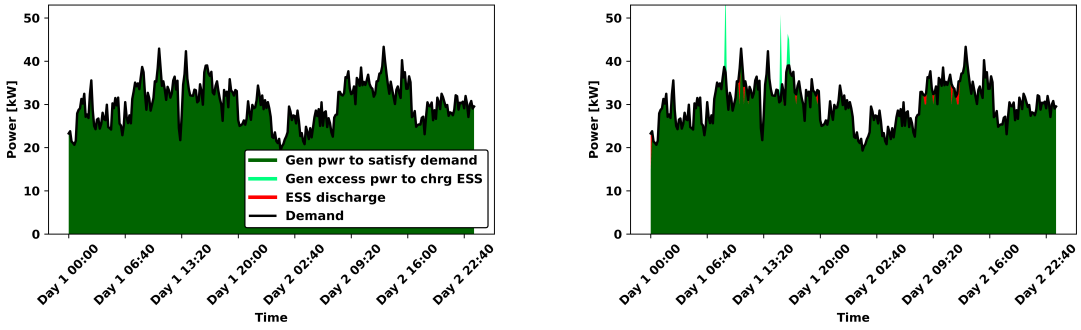

(a) Architecture without ESS

(b) Architecture with ESS

Figure 4.10. Power output plot for summer demand without ESS (left) and with ESS (right).

Table 4.6. Optimal fuel consumption and power output for the summer demand scenario with and without ESS.

Architecture	**Cumulative Fuel Consumption [gal]**	**Demand met by Generator [%]**	**Demand met by ESS [%]**	**Generator output used to charge ESS [%]**
Without ESS	170.18	100	0	0
With ESS	170.87	94.53	5.47	5.95

4.3.2 Linear Penalty

Next, we again consider a linear penalty term with coefficients of 0.2 gal/Δ, 0.4 gal/Δ, 0.6 gal/Δ, and 0.8 gal/Δ. Figure 4.11 shows the optimal power production for each of these coefficients, solved to a 1% optimality gap. As the figure indicates, most of the demand is satisfied by the generator, similar to Figure 4.6. Again, rapid generator fluctuations decrease substantially when any of the penalties is imposed, and the decrease is larger for a higher penalty coefficient.

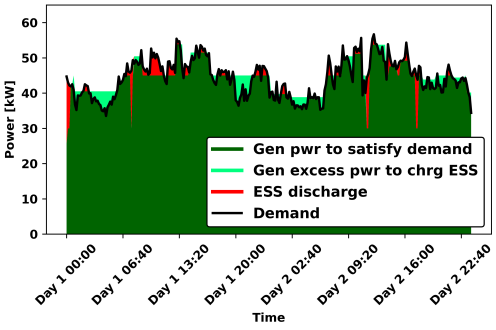

(a) 0.2 gal/Δ linear penalty coefficient

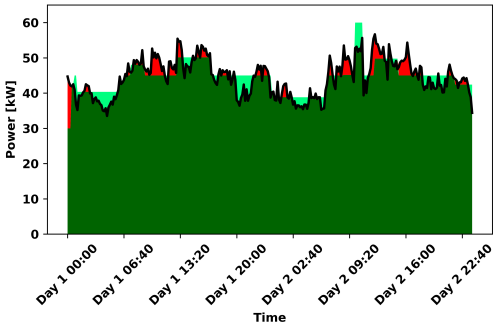

(b) 0.4 gal/Δ linear penalty coefficient

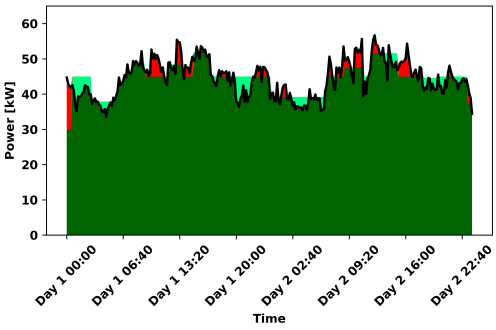

(c) 0.6 gal/Δ linear penalty coefficient

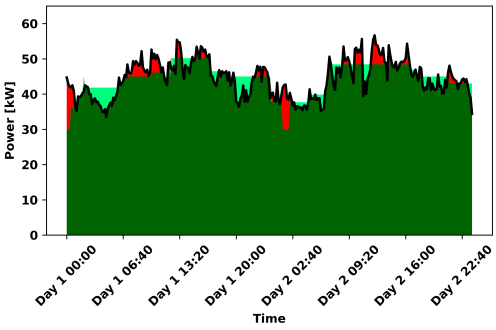

(d) 0.8 gal/Δ linear penalty coefficient

Figure 4.11. Power output plot based on linear penalties imposed on the generator for the summer demand scenario.

Mirroring Figure 4.11, Table 4.7 summarizes the results for each of the four penalty slope coefficients. As in the winter demand scenario, we observe that the presence of a penalty significantly impacts the overall breakdown of power production, while the exact value of the penalty does not significantly affect this breakdown, for the penalty values we consider.

Table 4.7. Optimal fuel consumption and power output with various linear penalties for the summer demand scenario.

Penalty	**Cumulative Fuel Consumption [gal]**	**Demand met by Generator [%]**	**Demand met by ESS [%]**	**Generator output used to charge ESS [%]**
No Penalty	170.87	94.53	5.47	5.95
Linear 0.2	171.47	97.23	2.77	2.92
Linear 0.4	171.30	97.08	2.92	3.11
Linear 0.6	171.71	97.14	2.81	3.05
Linear 0.8	171.86	96.85	3.15	3.37

4.3.3 Piecewise Linear Penalty

Finally, we again consider the four piecewise linear penalty functions shown in Figure 3.5 and display the optimal solution for each of these four cases in Figure 4.12. Again, the changes in generator and ESS optimal power production are minimal across the four piecewise linear penalty variations. Most of the demand is satisfied by the generator, as the dark green dominates the surface area of each plot. Additionally, the fluctuation in generator power output and ESS discharge rate decreases when the piecewise linear initial slope increases across the four penalties. Again, when the generator exceeds the demand, the additional power is charged into the ESS for future use.

Mirroring the graphical results, Table 4.8 depicts the corresponding numerical results for each of the different piecewise linear penalties. The results across the four piecewise linear penalties indicate that about 3% of the demand is satisfied by the ESS. The results display a consistent pattern of the generator supplying most of the demand. Again, the numerical results from the table reveal that the weight of the piecewise linear penalty coefficient is insignificant, as the generator and ESS scheduling power patterns are consistent across the four penalty variations.

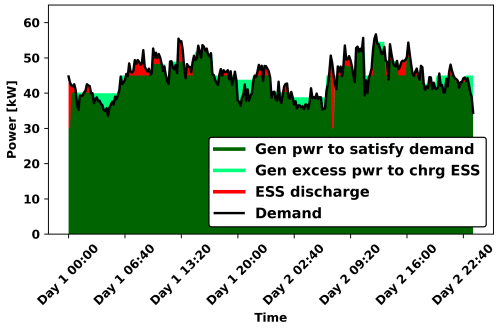

(a) 0.1 gal/Δ initial slope coefficient

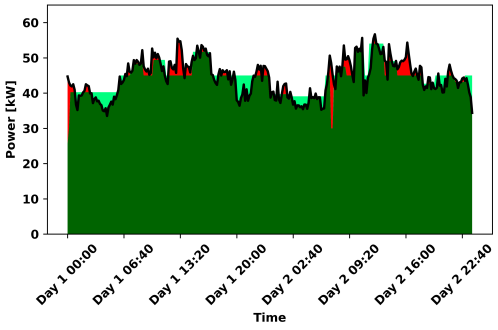

(b) 0.2 gal/Δ initial slope coefficient

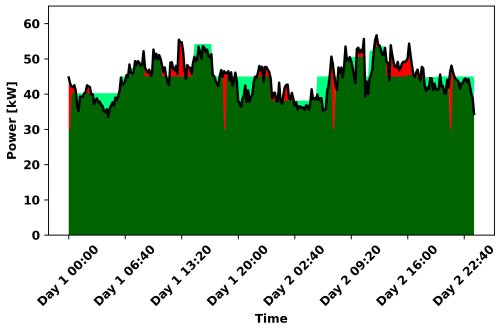

(c) 0.3 gal/Δ initial slope coefficient

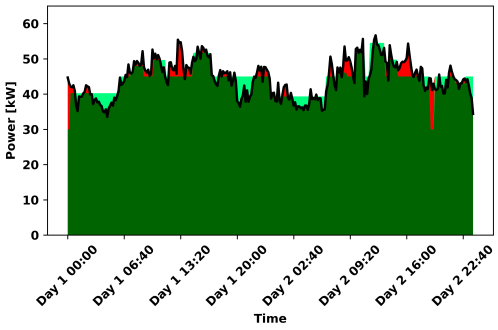

(d) 0.4 gal/Δ initial slope coefficient

Figure 4.12. Power output plot based on piecewise linear penalties imposed on the generator for the summer demand scenario.

Table 4.8. Optimal fuel consumption and power output with various piecewise linear penalties for the summer demand scenario.

Penalty	**Cumulative Fuel Consumption [gal]**	**Demand met by Generator [%]**	**Demand met by ESS [%]**	**Generator output used to charge ESS [%]**
No Penalty	170.87	94.53	5.47	5.95
Pi. Lin. 0.1	170.76	97.47	2.53	2.69
Pi. Lin. 0.2	171.06	97.21	2.79	2.93
Pi. Lin. 0.3	171.78	96.73	3.27	3.50
Pi. Lin. 0.4	171.69	97.12	2.88	3.07

Similar to Figure 4.8, Figure 4.13 also reiterates the importance of imposing a penalty on the generator. Likewise, the ESS is utilized more when a penalty is imposed on the generator, as optimization smooths out the generator power output to minimize cumulative fuel consumption.

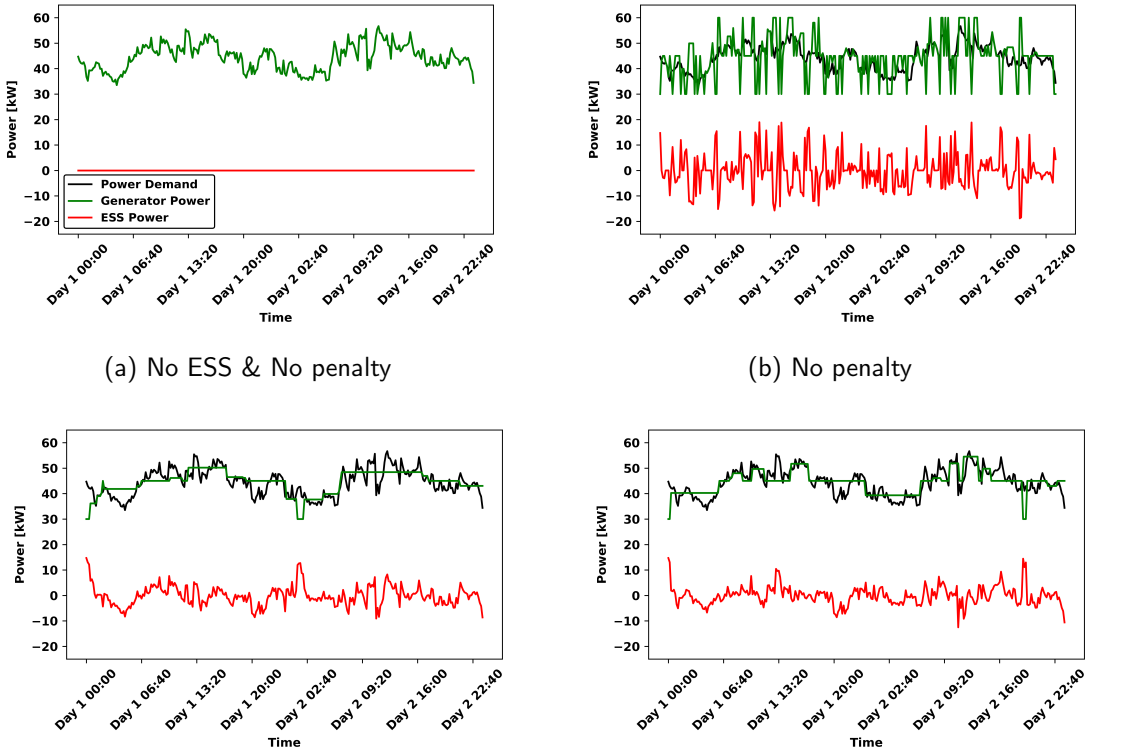

(a) No ESS & No penalty

(b) No penalty

(c) 0.8 gal/Δ linear penalty coefficient

(d) 0.4 gal/Δ initial slope piecewise linear coefficient

Figure 4.13. Optimal power distribution over various architectures for the summer demand scenario.

4.4 ESS Round Trip Efficiency Experimentation

The generator and ESS optimal power production varies drastically between the scenario with a penalty imposed on the generator and a scenario without a penalty imposed on the generator. In general, the activity of the ESS increases significantly when a penalty is imposed on the generator. In all previous scenarios, the ESS is set to a 90% RTE, consistent

with the research outlined in Chapter 2. While technological advancement may increase the ESS RTE above 90%, the price of the ESS exponentially increases as the RTE increases. This is a very important factor in microgrid design.

We now determine the impact of the ESS RTE on the overall fuel consumption of the generator over ten 24-hour demand scenarios. We are particularly interested in the fuel consumption change as ESS RTE decreases. Since a lower RTE is often cheaper to obtain, this study shows possible effects and trade offs that designers would have to make when selecting an ESS for their respective microgrid architecture. This study examines power demand scenarios during the winter months and the summer months to ensure that the overall power demand increase from the winter season to summer season of 15–20 kW is captured in the analysis.

4.4.1 Winter Season Case Study

Figure 4.14 exhibits the optimization results for the six different ESS RTEs spanning between 70% and 95% with four different piecewise linear penalties imposed on the generator. Each respective model is optimized over ten unique 24-hour demand scenarios during the winter season. We examine the cumulative fuel consumption at each ESS RTE across 240 distinct scenarios, shown as circular markers in the resulting figure.

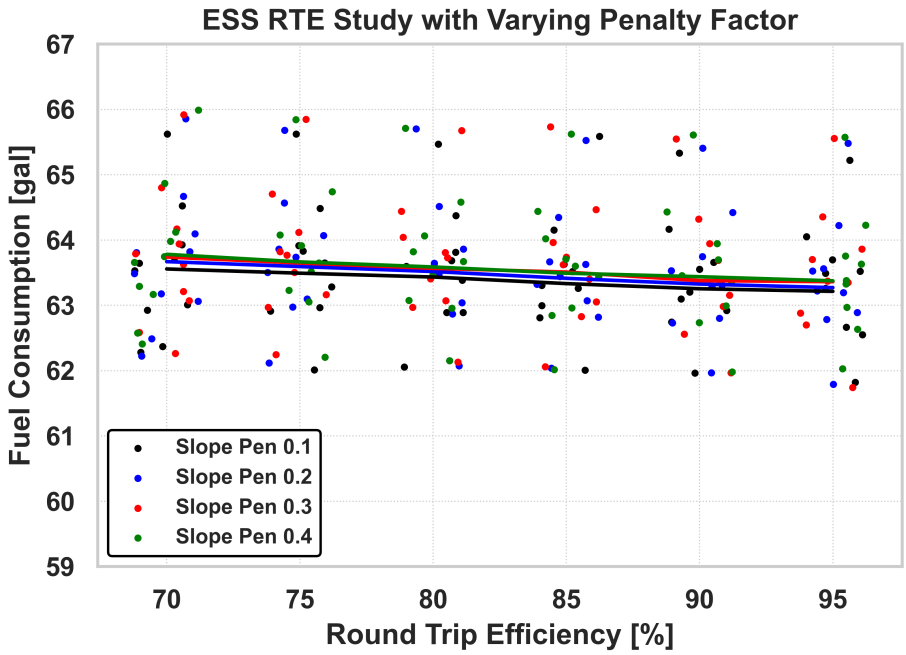

Figure 4.14. Fuel consumption results based on ESS RTEs optimized for the winter demand scenario.

The results of these 240 scenarios indicate an insignificant change in cumulative fuel consumption when the ESS RTE increases from 70% to 95% during the winter season. Each marker in Figure 4.14 shows a unique combination of a 24-hour demand scenario and a piecewise linear penalty based on an initial slope from a pool of ten different power demand scenarios and four piecewise linear penalty terms imposed on the generator. The four continuous lines show the cumulative fuel consumption of the ten power demand scenarios for each of the four piecewise linear penalty variations at each respective ESS RTE. The fuel consumption, on average, varies only slightly across the four piecewise linear penalty values, as well as across the six ESS RTE values. There is only a 1% decrease in cumulative fuel consumption between 70% and 95% RTE.

4.4.2 Summer Season Case Study

We conduct a similar ESS RTE study using summer season demand data. This data shows an increase of, on average, 15–20 kW over the winter demand. Figure 4.15 shows the opti-

mization results with the same input parameters as Figure 4.14; however, the ten distinctive 24-hour demand profiles originate from the summer season.

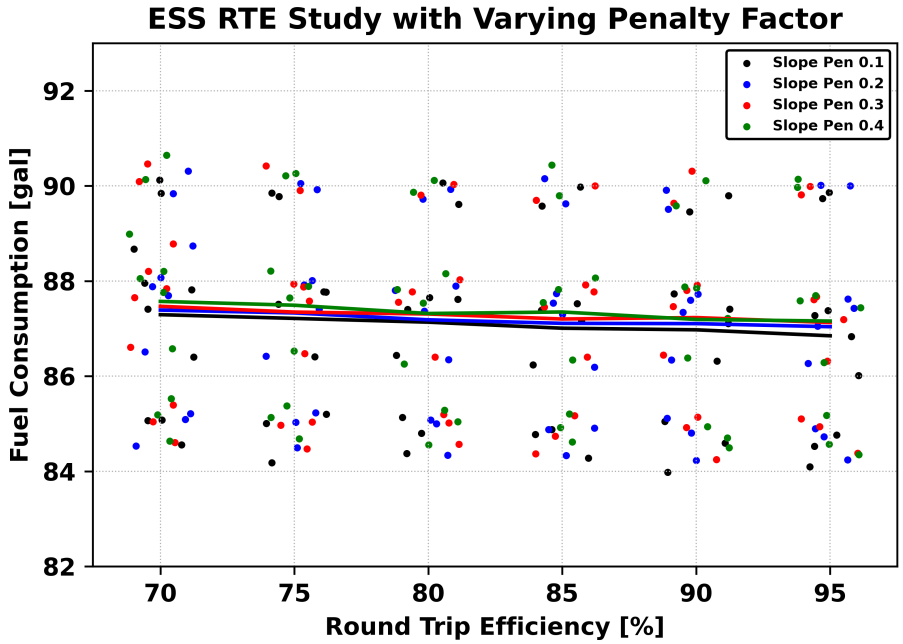

Figure 4.15. Fuel consumption results based on ESS RTEs optimized over summer demand.

The results shown in Figure 4.15 indicate a similar cumulative fuel consumption pattern across the six RTE values as observed with the winter demand data. Again, the cumulative fuel consumption across the RTE values varies by approximately 1–2 gal/day. This case study shows that for the parameters we considered, there is an insignificant change in fuel consumption as ESS RTE increases when the power demand increases, on average, 15–20 kW of power.

CHAPTER 5:
Conclusion

This thesis formulates a MILP optimization model that prescribes optimal generator and ESS usage to minimize fuel consumption while satisfying demand. A novel feature of this model is that it includes a penalty on generator output fluctuations. This penalty represents additional fuel that is consumed when the generator's output varies over time, and it has not been modeled in prior research. The inputs to the optimization model include a power demand scenario as well as the relevant characteristics of the generator, ESS, and penalty function.

We also exercise the MILP on case studies derived from actual FOB demand data. Our results indicate that an ESS is critical to achieving a smooth generator operating profile. However, in the absence of a penalty term, inclusion of an ESS actually results in *more* generator output fluctuations, compared to a microgrid architecture with no ESS. When a penalty term is included in the objective function, we observe much smoother generator output profiles, with peak loads satisfied by the ESS and excess generator power used to charge the ESS during periods of low demand. This results in modest immediate fuel savings and can be expected to lengthen the operational lifetime of the generator, an important consideration in practice. We observe only minimal changes in our optimal solutions as we vary the magnitude of the penalty term, indicating that the presence of a penalty term is more important than its exact magnitude, for the values we consider.

5.1 Future Work

While our MILP provides important insights on the impact of the penalty term on the optimal generator output profile and the resulting fuel consumption, it is not appropriate for implementation in a microgrid. The primary reason for this is that the MILP requires a complete demand profile as an input; it is thus "omniscient" and not suitable for real-time operation, where future demands are unknown. Thus, a natural next step for future research is to develop a real-time controller that attempts to replicate the smooth operating profiles observed in our optimal solutions. The real-time controller should take the past and present

power demand data to estimate and predict the future loads, possibly using an approach such as machine learning. With a successful real-time controller, the power system would be able to optimally manage time-varying load scenarios by using the ESS to satisfy unexpected fluctuating power demands.

Our model excursions consider a simple microgrid architecture and demand data based on a U.S. FOB in the Middle East. A crucial step is to alter the microgrid architectures by implementing different generators of varying sizes or even modifying the discharging and charging rates of the ESS, as well as exploring additional demand scenarios. It is critical to explore multiple microgrid architectures when varying locations have different resources and technologies available. Most microgrids used in operational FOBs include multiple generators with varying power production capacities, as well as many types and quantities of ESS, such as small and large capacity batteries. The transition to hybrid architectures is increasing as more renewable power generators such as PV cells and wind turbines are integrated into the microgrid in addition to the traditional diesel generators. An increase in sophisticated research shows that load scheduling algorithms are especially important to maximize fuel efficiency when fluctuating demand in the future can be planned in advance. The optimization model introduced in this thesis is an example of a microgrid model that can be modified based on the architecture types.

With the initial exploration of generator penalty terms using a simple microgrid optimization model, this thesis shows that a simple penalty term imposed on the generator has a significant influence on the optimal solution and overall fuel consumption. Due to the lack of empirical real-world data, our penalty terms are only notional. Further studies in the field are needed to examine the effect of time-varying loads on generator efficiency. These studies will lead to more realistic penalty terms that can optimally distribute power between the generator and ESS more accurately.

APPENDIX: Optimization Formulation

A.1 FOB Model with Linear Piecewise Penalty

Sets & Indices:

$t \in T = \{0, 10, 20, 30, ..., T\}$	Time periods
$i \in I = \{0, 1, 2, 3, 4\}$	Generator operating region (for linearization purposes)
$h \in H = \{0, 1, 2, 3, 4\}$	Generator fractional change regions (for linearization purposes)

Parameters:

sl^b	Generator base fuel consumption slope [gal/kW]
in^b	Generator base fuel consumption intercept [gal]
$demand_t$	Load that is demanded in time step t [kW]
l_i	Start of fractional change region i [kW]
u_i	End of fractional change region i [kW]
lo_h	Lower boundary of penalty region h [Δ]
up_h	Upper boundary of penalty region h [Δ]
slo_h	Slope of penalty function in region h [gal/Δ]
int_h	Intercept of penalty function in region h [gal]
dt	Time step [hours]
$battcap$	Battery capacity [kWh]
$effd$	Discharge efficiency of battery
$effc$	Charge efficiency of battery
$maxCharge$	Maximum battery rate of charge [kW]
$maxDischarge$	Maximum battery rate of discharge [kW]
$minGen$	Minimum generator load [kW]
$maxGen$	Maximum generator load [kW]
$minSOC$	Minimum battery state of charge [%]
$maxSOC$	Maximum battery state of charge [%]

Decision Variables:

gen_t	Continuous (≥ 0)	Generator power flow in time step t [kW]
$cbatt_t$	Continuous (≥ 0)	Power flow used to charge battery in time step t [kW]
$dbatt_t$	Continuous (≥ 0)	Power flow out of battery in time step t [kW]
SOC_t	Continuous (≥ 0)	Battery state of charge in time step t [%]
abs_chg_t	Continuous (≥ 0)	Absolute difference in generator power flow between time step $t-1$ and t [kW]
$Y_{i,t}$	Binary	1 if gen_t in region i in time step t and 0 otherwise
$P_{i,t}$	Continuous (≥ 0)	Auxiliary variable used for linearization: $P_{i,t} = Y_{i,t} abs\_chg_t$ [kW]
$frac\_chg_t$	Continuous (≥ 0)	Fractional [0-1] change in generator power flow between time step $t-1$ and t
$Y_{i,t}$	Binary	1 if $frac\_chg_t$ in region h in time step t and 0 otherwise
$Q_{h,t}$	Continuous (≥ 0)	Auxiliary variable used for linearization: $Q_{h,t} = W_{h,t} frac\_chg_t$

Objective Function:

$$\min \sum_{t \in T} \left[sl^b gen_t + in^b + \sum_{h \in H} \left(slo_h Q_{h,t} + int_h W_{h,t} \right) \right]$$

Constraints:

$$demand_t = gen_t + effd \cdot dbatt_t - cbatt_t \qquad \forall\, t \in T$$

$$minGen \le gen_t \le maxGen \qquad \forall\, t \in T$$

$$SOC_t = SOC_{t-1} - dbatt \cdot \frac{dt}{battcap} + effc \cdot cbatt_t \cdot \frac{dt}{battcap} \qquad \forall\, t \in T$$

$$0 \le dbatt_t \le maxDischarge \qquad \forall\, t \in T$$

$$0 \le cbatt_t \le maxCharge \qquad \forall\, t \in T$$

$$minSOC \le SOC_t \le maxSOC \qquad \forall\, t \in T$$

$$SOC_0 = SOC_T$$

$$gen_t - gen_{t-1} \le abs\_chg_t \qquad \forall\, t \in T$$

$$gen_{t-1} - gen_t \le abs\_chg_t \qquad \forall\, t \in T$$

$$0 \le P_{i,t} \le Y_{i,t}(maxGen - minGen) \qquad \forall\, i \in I, t \in T$$

$$abs\_chg_t - (maxGen - minGen)(1 - Y_{i,t}) \le P_{i,t} \le abs\_chg_t \qquad \forall\, i \in I, t \in T$$

$$\sum_{i \in I} Y_{i,t} l_i \le gen_t \le \sum_{i \in I} Y_{i,t} u_i \qquad \forall\, t \in T$$

$$\sum_{i \in I} \frac{2P_{i,t}}{l_i + u_i} = frac\_chg_t \qquad \forall\, t \in T$$

$$\sum_{h \in H} W_{h,t} lo_h \le frac\_chg_t \le \sum_{h \in H} W_{h,t} up_h \qquad \forall\, t \in T$$

$$0 \le Q_{h,t} \le up_{|H|} W_{h,t} \qquad \forall\, h \in H, t \in T$$

$$frac\_chg_t - up_{|H|}(1 - W_{h,t}) \le Q_{h,t} \le frac\_chg_t \qquad \forall\, h \in H, t \in T$$

$$\sum_{i \in I} Y_{i,t} = 1 \qquad \forall\, t \in T$$

$$\sum_{h \in H} W_{h,t} = 1 \qquad \forall\, t \in T$$

$$Y_{i,t} \in \{0, 1\} \qquad \forall\, i \in I, t \in T$$

$$W_{i,t} \in \{0, 1\} \qquad \forall\, h \in H, t \in T$$

List of References

Ahmed M, Vahidnia A, Meegahapola L, Datta M (2017) Small signal stability analysis of a hybrid AC/DC microgrid with static and dynamic loads. *2017 Australasian Universities Power Engineering Conference (AUPEC)*, 1–6, URL http://dx.doi.org/10.1109/AUPEC.2017.8282414.

Bahramirad S, Reder W, Khodaei A (2012) Reliability-constrained optimal sizing of energy storage system in a microgrid. *IEEE Transactions on Smart Grid* 3(4):2056–2062, URL http://dx.doi.org/10.1109/TSG.2012.2217991.

Bhandari Y, Chalise S, Sternhagen J, Tonkoski R (2013) Reducing fuel consumption in microgrids using PV, batteries, and generator cycling. *IEEE International Conference on Electro-Information Technology , EIT 2013*, 1–4, URL http://dx.doi.org/10.1109/EIT.2013.6632692.

Bouaicha H, Craparo E, Dallagi H, Nejim S (2020) Dynamic optimal management of a hybrid microgrid based on weather forecasts. *Turkish Journal of Electrical Engineering & Computer Sciences* 28(4):2060–2076, URL http://dx.doi.org/10.3906/elk-1910-6.

Chen SX, Gooi HB, Wang MQ (2012) Sizing of energy storage for microgrids. *IEEE Transactions on Smart Grid* 3(1):142–151, URL http://dx.doi.org/10.1109/TSG.2011.2160745.

Craparo E, Karatas M, Singham DI (2017) A robust optimization approach to hybrid microgrid operation using ensemble weather forecasts. *Applied Energy* 201:135–147, ISSN 0306-2619, URL http://dx.doi.org/10.1016/j.apenergy.2017.05.068.

Craparo E, Sprague J (2019) Integrated supply- and demand-side energy management for expeditionary environmental control. *Applied Energy* 233-234:352–366, ISSN 0306-2619, URL http://dx.doi.org/10.1016/j.apenergy.2018.09.220.

del Valle Y, Venayagamoorthy GK, Mohagheghi S, Hernandez J, Harley RG (2008) Particle Swarm Optimization: Basic concepts, variants and applications in power systems. *IEEE Transactions on Evolutionary Computation* 12(2):171–195, URL http://dx.doi.org/10.1109/TEVC.2007.896686.

Department of Defense (2018) Summary of the 2018 National Defense Strategy of The United States of America. Accessed March 8, 2021, https://dod.defense.gov/Portals/1/Documents/pubs/2018-National-Defense-Strategy-Summary.pdf.

Fakhrazari A, Vakilzadian H, Choobineh FF (2014) Optimal energy scheduling for a smart entity. *IEEE Transactions on Smart Grid* 5(6):2919–2928, URL http://dx.doi.org/10.1109/TSG.2014.2319247.

Gamarra C, Guerrero JM (2015) Computational optimization techniques applied to microgrids planning: A review. *Renewable and Sustainable Energy Reviews* 48:413–424, ISSN 1364-0321, URL http://dx.doi.org/10.1016/j.rser.2015.04.025.

Garcia K (2017) *Optimization of microgrids at military remote base camps*. Master's thesis, Naval Postgraduate School, Monterey, CA, URL https://calhoun.nps.edu/handle/10945/56923.

Hartono BS, Budiyanto Y, Setiabudy R (2013) Review of microgrid technology. *2013 International Conference on QiR*, 127–132, URL http://dx.doi.org/10.1109/QiR.2013.6632550.

Hernandez-Aramburo CA, Green TC, Mugniot N (2005) Fuel consumption minimization of a microgrid. *IEEE Transactions on Industry Applications* 41(3):673–681, URL http://dx.doi.org/10.1109/TIA.2005.847277.

International Business Machines Corporation (IBM) (2009) IBM ILOG CPLEX Optimization Studio (CPLEX). URL https://www.ibm.com/products/ilog-cplex-optimization-studio.

Katiraei F, Abbey C (2007) Diesel plant sizing and performance analysis of a remote wind-diesel microgrid. *2007 IEEE Power Engineering Society General Meeting*, 1–8, URL http://dx.doi.org/10.1109/PES.2007.386275.

Katiraei F, Iravani MR, Lehn PW (2005) Micro-grid autonomous operation during and subsequent to islanding process. *IEEE Transactions on Power Delivery* 20(1):248–257, URL http://dx.doi.org/10.1109/TPWRD.2004.835051.

Kazem HA, Khatib T (2013) A novel numerical algorithm for optimal sizing of a photovoltaic/wind/diesel generator/battery microgrid using loss of load probability index. *International Journal of Photoenergy* 2013:1–8, URL http://dx.doi.org/10.1155/2013/718596.

Kiser E (2018) *The impact of technologies and missions on contingency base fuel consumption*. Master's thesis, Naval Postgraduate School, Monterey, CA, URL https://calhoun.nps.edu/handle/10945/59699.

Li H, Eseye AT, Zhang J, Zheng D (2017) Optimal energy management for industrial microgrids with high-penetration renewables. *Protection and Control of Modern Power Systems* 2(1):1–14.

Li K, Tseng KJ (2015) Energy efficiency of lithium-ion battery used as energy storage devices in micro-grid. *IECON 2015 - 41st Annual Conference of the IEEE Industrial Electronics Society*, 005235–005240, URL http://dx.doi.org/10.1109/IECON.2015.7392923.

Liu J, Huang X, Zuyi L (2020) Multi-time scale optimal power flow strategy for medium-voltage DC power grid considering different operation modes. *Journal of Modern Power Systems and Clean Energy* 8:46–54, URL http://dx.doi.org/10.35833/MPCE.2018.000781.

Majima M, Ujiie S, Yagasaki E, Koyama K, Inazawa S (2001) Development of long life lithium ion battery for power storage. *Journal of Power Sources* 101(1):53–59, ISSN 0378-7753, URL http://dx.doi.org/10.1016/S0378-7753(01)00554-7.

Moradi H, De Groff D, Abtahi A (2017) Optimal energy scheduling of a stand-alone multi-sourced microgrid considering environmental aspects. *2017 IEEE Power Energy Society Innovative Smart Grid Technologies Conference (ISGT)*, 1–5, URL http://dx.doi.org/10.1109/ISGT.2017.8086013.

Morstyn T, Hredzak B, Aguilera RP, Agelidis VG (2018) Model predictive control for distributed microgrid battery energy storage systems. *IEEE Transactions on Control Systems Technology* 26(3):1107–1114, URL http://dx.doi.org/10.1109/TCST.2017.2699159.

Moseley PT, Garche J (2015) Chapter 4: Applications and markets for grid-connected storage systems. Moseley PT, Garche J, eds., *Electrochemical Energy Storage for Renewable Sources and Grid Balancing*, 440–443 (Amsterdam: Elsevier), ISBN 978-0-444-62616-5, URL http://dx.doi.org/10.1016/B978-0-444-62616-5.05001-4.

Office of the Assistant Secretary of Defense for Energy, Installations, and Environment (2018a) New operational energy strategy released by the department. Accessed March 6, 2021, https://www.acq.osd.mil/eie/OE/OE%20Strategy%20Page.html.

Office of the Assistant Secretary of Defense for Energy, Installations, and Environment (2018b) Operational energy. Accessed March 8, 2021, https://www.acq.osd.mil/eie/OE/OE%20Strategy%20Page.html.

Singleton B (2017) US Army Base Camp Integration Lab. Email exchanges and site visit.

Sprague G John (2015) *Optimal scheduling of time-shiftable electric loads in expeditionary power grids*. Master's thesis, Naval Postgraduate School, Monterey, CA, URL https://calhoun.nps.edu/handle/10945/47332.

Ton D, Reilly J (2017) Microgrid controller initiatives: An overview of RD by the U.S. Department of Energy. *IEEE Power and Energy Magazine* 15(4):24–31, URL http://dx.doi.org/10.1109/MPE.2017.2691238.

Ulmer N (2014) *Optimizing microgrid architecture on Department of Defense installations*. Master's thesis, Naval Postgraduate School, Monterey, CA, URL https://calhoun.nps.edu/handle/10945/44023.

United States Army Acquisition Support Center (2017) Advanced Medium Mobile Power Source (AMMPS). Accessed March 23, 2021, https://asc.army.mil/web/portfolio-item/cs-css-advanced-medium-mobile-power-source-ammps/.

United States Code (2018) 10 U.S.C. §2924: Definition.

Initial Distribution List

1. Defense Technical Information Center
   Ft. Belvoir, Virginia

2. Dudley Knox Library
   Naval Postgraduate School
   Monterey, California